Multi-energy microgrids

An optimal despatch model for water-energy nexus

Jalilian, Faezeh ; Mirzaei, Mohammad Amin ; Zare, Kazem; Mohammadi-Ivatloo, Behnam ; Marzband, Mousa; Anvari-Moghaddam, Amjad

Published in:
Sustainable Cities and Society

DOI (link to publication from Publisher):
10.1016/j.scs.2021.103573

Publication date:
2022

Document Version
Publisher's PDF, also known as Version of record

Sustainable Cities and Society 77 (2022) 103573

Contents lists available at ScienceDirect

Sustainable Cities and Society

journal homepage: www.elsevier.com/locate/scs

Multi-energy microgrids: An optimal despatch model for water-energy nexus

Faezeh Jalilian [a], Mohammad Amin Mirzaei [a], Kazem Zare [a,*], Behnam Mohammadi-Ivatloo [a,c], Mousa Marzband [b], Amjad Anvari-Moghaddam [a,c]

[a] Faculty of Electrical and Computer Engineering, University of Tabriz, Tabriz, Iran
[b] Northumbria University, Electrical Power and Control Systems Research Group, Ellison Place NE1 8ST Newcastle upon Tyne, United Kingdom
[c] Integrated Energy Systems Laboratory, Department of Energy Technology, Aalborg University, 9220 Aalborg, Denmark

ARTICLE INFO

Keywords:
Energy-water nexus
Multi-energy microgrid
Energy storage systems
Multi-objective optimization
Two-stage stochastic programming

ABSTRACT

This paper proposes an integrated scheduling model for optimal despatch of cooling, heating, power, gas and water sources in an energy-water microgrid, where the microgrid operator participates in the power, heat, and gas markets and utilizes energy conversion facilities to meet various demands. Further, the role of water and energy storage systems (WESSs) and demand response program (DRP) is investigated on optimal scheduling of the combined cooling, heating, power, gas, and water-based microgrid. In addition, a multi-objective two-stage stochastic optimization model is adopted to minimize the total cost, including operating and emission costs and the amount of potable water extracted from water wells due to the uncertainties of electrical demand, wind power, and electricity market price. Moreover, the epsilon-constraint method and fuzzy satisfying approach are applied to obtain the optimal solution in the multi-objective problem. Ultimately, the simulation results confirm the advantages of simultaneous consideration of WESSs and DRP on the total cost of the proposed energy-water microgrid.

1. Introduction

1.1. Overview

In recent years, due to problems such as scarcity of conventional energy resources and the ageing of the electricity network infrastructure, the power system has faced challenges. Generating power and supplying different loads through locally available renewable energy sources (RESs) have led to the appearance of a novel concept named microgrid (MG). In fact, the MG is a small-scale power system that can meet consumers' energy and works in different operation modes (grid-connected and islanded) (Hemmati, Mohammadi-Ivatloo, Ghasemzadeh & Reihani, 2018; Mansour-Saatloo, Mirzaei, Mohammadi-Ivatloo & Zare, 2020b). With the integration of RESs into a microgrid like boilers, combined heat and power (CHP) units and chillers, multi-energy microgrids (MEMGs) can be formed. This structure has advantages like mitigating carbon emissions, reducing costs and increasing efficiency through leveraging an integrated energy system model. The MEMG can meet thermal, electrical and cooling loads simultaneously (Mansour-Saatloo et al., 2020b; Pourghasem, Sohrabi, Abapour & Mohammadi-Ivatloo, 2019). Co-/tri-generation systems in MEMG can increase power generation by about 30% in power plants, while reducing greenhouse gas emission by approximately 13–18%, which denote the economic and environmental benefits of such energy sources (Wu, Wang, Fu & Xu, 2017). On the other hand, economic development together with rapid population growth and urbanization significantly affect vital resources, such as energy and water. The energy and water crisis is one of the critical problems in the future with increasing demand, increasing scales, climate change and natural disasters (Dai et al., 2018). According to statistics, energy and water demands will grow by about 40% and 30%, respectively, by 2035 (Li et al., 2019). Energy and water systems are inextricably interdependent. Water can be utilized to produce and consume energy in different stages, while energy can be used to extract, deliver, distribute, and treat water (Shang et al., 2018). Thus, to enable an efficient energy-water nexus, integrated approaches can be used to scheduling and operate water and energy systems through the so-called energy-water microgrids (EWMG) (Moazeni & Khazaei, 2020a).

* Corresponding author.
E-mail address: kazem.zare@tabrizu.ac.ir (K. Zare).

https://doi.org/10.1016/j.scs.2021.103573
Received 17 June 2021; Received in revised form 8 November 2021; Accepted 9 November 2021
Available online 24 November 2021

Nomenclature

Indices

t, τ	Time interval
j	CHP units
w	Scenario

Parameters

N_t	Total of period time
N_j	Total of CHP units
N_w	Total of scenarios
C_j^{su}/C_j^{sd}	Start-up/shut-down cost of CHP units ($/kWh)
$C^{EL,dn}/C^{EL,up}$	Increase/decrease cost of electrical demand ($/kWh)
DRE	Adjustable electrical load value (%)
ρ_w	Occurrence probability of scenario
$ED_{t,w}$	Electrical demand (kW)
$HD_t/GD_t/CD_t/WD_t$	Heat/gas/cooling/water demand (kW)
$ED_{t,w}^{DR}$	The value of electrical demand after the applying DR program (kW)
$P_{t,w}^{wind}$	The power generated via wind turbine (kW)
$\lambda_{t,w}^{EM}$	Electricity market price ($/kWh)
λ_t^{HM}	Heat market price ($/kWh)
λ_t^{GM}	Gas market price ($/kWh)
λ^C	Carbon price ($/kg)
α, β, γ	Carbon emission coefficient (kg/kWh)
K	Positive constant
CS	Cross-section of WST (m^2)
$LS^{\max}$	Maximum capacity of WST (m)
L^{WL}	Level of Water well (m)
L^G	The height of WST (m)
g	Gravity (m^2/h)
φ	Water density (kg/m^3)
T_j^{ON}/T_j^{OFF}	Minimum on/off time of the CHP units (h)
η_j	The efficiency of CHP units
$H^{gb,\max}/H^{gb,\min}$	Max/min capacity of gas boiler (kW)
$H^{eb,\max}/H^{eb,\min}$	Max/min capacity of electric boiler (kW)
$E^{HS,\max}/E^{HS,\min}$	Max/min level of HSS (kWh)
$E^{HS,ch,\max}/E^{HS,disch,\max}$	Maximum charging/discharging of HSS (kW)
$E^{GS,\max}/E^{GS,\min}$	Max/min level of GSS (kWh)
$P^{ch,GS,\max}/P^{ch,GS,\min}$	Max/min charging of GSS (kW)
$P^{disch,GS,\max}/P^{disch,GS,\min}$	Max/min discharging of GSS (kW)
$E^{ES,\max}/E^{ES,\min}$	Max/min level of ESS (kWh)
$P^{ch,ES,\max}/P^{ch,ES,\min}$	Max/min charging of ESS (kW)
$P^{disch,ES,\max}/P^{disch,ES,\min}$	Max/min discharging of ESS (kW)
$E^{ISS,\max}/E^{ISS,\min}$	Max/min level of ISS (kWh)
$P^{ch,ISS,\max}/P^{ch,ISS,\min}$	Max/min charging of ISS (kW)
$P^{disch,ISS,\max}/P^{disch,ISS,\min}$	Max/min discharging of ISS (kW)
$C^{abchlr,\max}/C^{abchlr,\min}$	Max/min capacity of absorption chiller (kW)
$Q^{S,ch,\max}/Q^{S,disch,\max}$	Maximum charging/discharging of WST (m^3/h)
$Q^{D,\max}$	Maximum capacity of SDS (m^3/h)
η^{gb}	The efficiency of gas boiler
η^{eb}	The efficiency of electrical boiler
η^{HS}	The efficiency of HSS
$\eta^{HS,ch}/\eta^{HS,disch}$	The efficiency of HSS charge/discharge
$\eta^{ch,GS}/\eta^{disch,GS}$	The efficiency of GSS charge/discharge
$\eta^{ch,ES}/\eta^{disch,ES}$	The efficiency of ESS charge/discharge
$\eta^{ch,ISS}/\eta^{disch,ISS}$	The efficiency of ISS charge/discharge
η^{abchlr}	The efficiency of absorption chiller
η^{PWL}	The efficiency of water well pump
η^{PS}	The efficiency of WST pump
η^D	The energy efficiency of SDS

Variables

$dr_{t,w}^{EL,up}, dr_{t,w}^{EL,dn}$	Changes of the electrical demand after applying the demand response program (kW)
$P_{t,w}^{EM,imp}/P_{t,w}^{EM,sell}$	Imported/sold power from/to the main grid (kW)
$P_{t,w}^{HM,imp}/P_{t,w}^{HM,sell}$	Imported/sold heat from/to the main grid (kW)
$P_{t,w}^{GM,imp}$	Imported gas from the main grid (kW)
$P_{t,w,j}$	The power generated via CHP units (kW)
$H_{t,w,j}$	The heat generated via CHP units (kW)
$GC_{t,w,j}$	Gas consumed via CHP units (kW)
$GB_{t,w}^{gb}$	Gas consumed via gas boiler (kW)
$H_{t,w}^{gb}$	The heat generated via gas boiler (kW)
$EB_{t,w}^{eb}$	Power consumed via electric boiler (kW)
$H_{t,w}^{eb}$	The heat generated via electric boiler (kW)
$E_{t,w}^{HS}$	Charge level of HSS (kWh)
$E_{t,w}^{GS}$	Charge level of GSS (kWh)
$E_{t,w}^{ES}$	Charge level of ESS (kWh)
$E_{t,w}^{ISS}$	Charge level of ISS (kWh)
$H_{t,w}^{HS,ch}/H_{t,w}^{HS,disch}$	Charge/discharge of HSS (kW)
$P_{t,w}^{ch,GS}/P_{t,w}^{disch,GS}$	Charge/discharge of GSS (kW)
$P_{t,w}^{ch,ES}/P_{t,w}^{disch,ES}$	Charge/discharge of ESS (kW)
$P_{t,w}^{ch,ISS}/P_{t,w}^{disch,ISS}$	Charge/discharge of ISS (kW)
$C_{t,w}^{abchlr}$	The cooling generated by absorption chiller (kW)
$H_{t,w}^{abchlr}$	Heat consumed by absorption chiller (kW)
$Q_{t,w}^{WL}$	Water extracted from the well (m^3/h)
$Q_{t,w}^{D}$	Water generation by SDS (m^3/h)
$Q_{t,w}^{S,ch}/Q_{t,w}^{S,disch}$	Charging/discharging amount of WST (m^3/h)
$LS_{t,w}$	The water level of WST (m)
$P_{t,w}^{PWL}$	Power consumed by water well pump (kW)
$P_{t,w}^{PS}$	Power consumed by WST pump (kW)
$P_{t,w}^{D}$	Power consumed by SDS (kW)
$P_{t,w}^{water}$	Total power consumed by water network (kW)

Binary variables

$I_{t,j}$	On/off state of the CHP units
$V_{1,t}/V_{2,t}$	Operating point status of the second type CHP unit in the first/second convex sector of FOR
$Y_{t,j}/Z_{t,j}$	Start-up/shut-down of CHP units
$I_{t,w}^{gb}$	On/off state of the gas boiler
$I_{t,w}^{eb}$	On/off state of the electric boiler
$I_{t,w}^{HS,ch}/I_{t,w}^{HS,disch}$	Charging/discharging state of HSS
$I_{t,w}^{ch,GS}/I_{t,w}^{disch,GS}$	Charging/discharging state of GSS
$I_{t,w}^{ch,ES}/I_{t,w}^{disch,ES}$	Charging/discharging state of ESS
$I_{t,w}^{ch,ISS}/I_{t,w}^{disch,ISS}$	Charging/discharging state of ISS
$I_{t,w}^{S,ch}/I_{t,w}^{S,disch}$	Charging/discharging state of WST

1.2. Literature review

Some studies have evaluated the optimization operation and management of the microgrids. A bidding strategy for microgrids has been presented in Mirzaei et al. (2020a) using a two-stage bi-level programming, where the capability to reconfiguration microgrids is considered to maximize microgrid profit. A novel index for reconfigurable microgrids islanding operation has been introduced in Hemmati, Mohammadi-Ivatloo, Abapour and Anvari-Moghaddam (2020), which is called the probability of islanding operation and represents the ability of the microgrid to meet load demand, where chance-constrained scheduling for the reconfigurable microgrid is presented to minimize costs. In Daneshvar et al. (2020) various models for microgrids participation in the energy trading market have been proposed by considering the concept of transactive energy to handle power trading in the network and in the presence of uncertainties. The decision-making structure of distribution networks (including MGs and retailers) has been presented in Fateh, Bahramara and Safari (2020), in which through a proposed structure for energy exchange with the market, MGs and retailers can optimize related goals. In Hou et al. (2020), a multi-objective problem for MG economic operation with electric vehicles, shiftable loads and generators has been introduced, where the operating cost of the microgrid, utilization rate of photovoltaic energy and the power oscillation between the microgrid and the main network are considered as objectives. The optimization of power exchanging in reconfigurable microgrids by considering distributed energy resources has been investigated in Jahani, Zare, Khanli and Karimipour (2021).

Besides the microgrids problem, the concept of the MEMGs has attracted much attention, so that researchers have investigated it under different approaches. An optimal multi-objective problem for multi-carrier microgrids energy management has been employed to minimize cost and decrease losses and carbon emission rate (Murty & Kumar, 2020). A stochastic-robust approach has been optimized for combined cooling, heating and power-based (CCHP) MGs in Y. Wang, Tang, Yang, Sun and Zhao (2020) to coordinate the optimization of CCHP microgrids and power exchange with the electricity market. Authors of (Cui et al., 2020) have investigated the significance and effects of modelling devices for the multi-objective operation of CCHP-based microgrids and shiftable load using a partial load ratio model. Optimal scheduling of MEMG integrated with RESs has been investigated in Saberi, Pashaei-Didani, Nourollahi, Zare and Nojavan (2019) to solve economic and environmental problems, in which real-time demand response (DR) is considered. In Amir and Azimian (2020), dynamic MEMGs development has been analysed using a dynamic MEMGs scheduling model. In Ding, Guo, Qiannan and Jermsittiparsert (2021) have been evaluated the environmental and economic effects of MEMGs under a robust/stochastic optimization approach to minimize costs and CO_2 emission rate. A temporally-coordinated approach for MEMG taking into account various energy properties has been represented in Li and Xu (2019) to coordinate diverse energies in the presence of uncertainties from RESs, electrical load, and prices. In Mansour-Saatloo et al. (2020a), the authors have focused on the concept of CHP-based microgrid by considering the integrated DR and hydrogen storage system. An integration structure of combined cooling, heating, power and gas-based (CCHPG) microgrid has been investigated in Yang, Tang, Wang and Sun (2020) to manage risk by considering operating cost control. In Nami, Anvari-Moghaddam and Arabkoohsar (2020), the waste heat and geothermal heat resources have been utilized in CCHP units to supply thermal and electrical demands, in which not only is provided energy demands but also surplus energy is delivered to the main grid. A scenario-based stochastic isolated MEMGs investment programming model has been introduced in Ehsan and Yang (2019) to minimize costs and emission under different uncertainties and demands. Likewise, the multi-period programming problem of MEMG has been studied in Wei, Zhang, Wang, Cao and Khan (2020a) taking into account long-term and short-term uncertainties.

Significant researches have also been made in the domain of integrated water and energy systems and their optimal management. In Pakdel, Sohrabi and Mohammadi-Ivatloo (2020), a multi-objective problem to decrease energy costs and groundwater extraction has been introduced, in which the concept of transactive energy is used to achieve further system flexibility. In Ahmadi, McLellan, Ogata, Mohammadi-Ivatloo and Tezuka (2020), an optimal scheduling to supply sustainable energy and water system has been presented, where a novel model is applied to investigate synergies and conflicts of the scheduling of both the energy and water systems simultaneously. An optimization method for minimizing energy consumption of the water system with variable and fixed speed pumps in the EWMG system has been demonstrated in Moazeni and Khazaei (2020b). A navel approach has been investigated in Feizizadeh et al. (2021) in order to sustainability evaluation of urban potable water usage patterns in Tabriz, where urban structure and population have a considerable effect on water usage. A comprehensive programming model have been presented to develop the resilience of water-power systems with microgrids, where the aim of the problem is to reduce the investment costs (Najafi, Peiravi, Anvari-Moghaddam & Guerrero, 2019). In Roustaei et al. (2020), a structure of scenario-based for EWMG to maintain the balance of multi-energy carriers and optimal programming for its infrastructure has been provided, where according to this programming, the total investment and environmental costs are minimized. A co-optimization approach of the islanded EWMG has been used to reduce energy usage in the water system and energy production cost at the energy system (Moazeni, Khazaei & Mendes, 2020). By using an environment-based input-output approach, the authors of (X.-C. Wang et al., 2020) have explored water-energy nexus while considering carbon emissions. In Zhang, Valencia, Gu, Zheng and Chang (2020), a novel strategy has been introduced to integrate the emerging and existing of the renewable energy resources into a community MG to improve community resilience, where an energy-water nexus model has been presented for sustainable system development. The contribution of the extended water-energy nexus (e.g., food, pollution, ground, waste and so on) to improve the environmental sustainability has been discussed in Wang et al. (2021). In Sui, Wei, Lin and Li (2021), the optimal management structure has been proposed with the integration of a MG and a water supply system to solve the problem of the water system flexibility. Two optimal models for an energy-water system have been observed in Moazeni and Khazaei (2021), which is to provide the optimal number and location of the pumps-as-turbines by one model and to minimize the energy production cost by another model. Authors of (Li, Yu, Al-Sumaiti & Turitsyn, 2018) have investigated the capability of the water system to provide DRP management to the power network with respect to the micro water-energy nexus structure.

1.3. Contribution

Based on the reviewed literature and the authors' best knowledge, the focus on combined cooling, heating, power, gas, and water-based microgrid (CCHPGW-MG) has been ignored. The significant gaps in the reviewed literature are described as follows:

- Some literature has only considered the optimal management and scheduling of microgrids e.g., (Daneshvar et al., 2020; Fateh et al., 2020; Hemmati et al., 2020; Hou et al., 2020; Jahani et al., 2021; Mirzaei et al., 2020a) and has ignored the effect of multi-energy microgrids, even though it is one of the essential research aspects.
- Numerous studies have investigated the impacts and benefits of multi-energy microgrids under different approaches e.g., (Ding et al., 2021; Ehsan & Yang, 2019; Murty & Kumar, 2020; Nami et al., 2020; Saberi et al., 2019; Wei, Zhang, Wang, Cao & Khan, 2020b), while disregarding the effect of energy-water microgrids. Nevertheless, the energy-water microgrids should gain prime attention because of the energy and water crisis.

- Most of the literature has investigated the scheduling of energy-water microgrids e.g., (Moazeni & Khazaei, 2020b; Moazeni et al., 2020; Roustaei et al., 2020; Wang et al., 2021; Zhang et al., 2020), while ignoring the optimal integrated scheduling of the energy-water microgrids to supply different demands.

Table 1 illustrates the comparison of the existing models in the reviewed literature with the proposed one in this study. As can be clearly observed, this paper presents a developed microgrid model under the concept of CCHPGW-MG, which meets different energy demands simultaneously via participating in multi-energy markets. The proposed model is formulated as a multi-objective problem that aims to minimize operating cost, emission cost, and the amount of potable water extracted from water wells, simultaneously. The ε-constraint method has been employed to solve the multi-objective problem, also the fuzzy approach is used to choose the optimal values of the objective functions. The DRP is considered to shift electrical demands from electricity price peak hours to electricity price off-peak hours and is reduce total operating cost. Moreover, a two-stage stochastic approach is also applied to manage uncertainties. The principal contributions of this work can be categorized as follows:

- An energy-water microgrid is introduced in this paper under the concept of CCHPGW-MG, in which the microgrid operator participates in multi-energy markets to provide various demands, including electricity, heating, cooling, gas and water.
- The effect of multiple storage systems, including electrical storage system (ESS), heat storage system (HSS), gas storage system (GSS), ice storage system (ISS), and water storage tank (WST), as well as DR program, is investigated on optimal scheduling of the proposed microgrid.
- Water system technologies, including seawater desalination system (SDS), well water and WST, is considered to supply water demand and increase water system flexibility.
- A two-stage stochastic approach is adopted to handle the uncertainties associated with electrical load, wind power and electricity price in the multi-energy microgrid.

The rest of the paper is organized as below: The structure of the CCHPGW-MG along with its details is given in Section 2. Section 3 introduces the problem formulation, including the objective functions, problem constraints, and the examined multi-objective optimization model. The simulation results are given in Section 4. Untimely, Section 5 concludes the paper.

2. Structure of CCHPGW-MG

Fig. 1 shows the structure of the CCHPGW-MG, energy sector technologies including electrical boiler, gas boiler, two types of CHP unit with various feasible operating regions (FORs), wind turbines, heat electrical storage system (ESS), storage system (HSS), gas storage system (GSS), ice storage system (ISS), absorption chiller and water sector technologies including seawater desalination system (SDS), water storage tank (WST) and well water. In this study, a two-stage stochastic approach is adopted to manage uncertainties associated with the electrical demand, wind power, and electricity market price in the proposed model. The first stage is associated with the start-up and shut-down costs of the CHP units, and the second stage corresponds to the scenarios related to the costs of operation and distribution of the energy and water systems technologies. The microgrid is fed by the upstream electricity, heating and gas networks, wind turbines, and water to meet various energy and water demands securely. As mentioned before, the water and energy crisis is one of the fundamental problems which has led researchers to investigate. The use of desalination technology solves the water shortage issue, but since eliminating salt from seawater consumes a lot of energy, so using this technology alone is not cost-effective. In addition, the reduction of groundwater freshwater reserves is another major problem. Therefore, simultaneous consideration of water system technologies such as SDS, WST, and water wells is a fundamental solution to solve the water and energy crisis.

- **Electrical sector:** According to Fig. 1, electricity demand, equipment input such as electrical boiler, ISS and water sector technologies is met by the upstream electricity network, CHP units, ESS and wind turbines. Furthermore, part of the power generated, in the hours when the electricity market price is high, sold to the electricity grid.
- **Heat sector:** Heat demand and absorption chiller input is supplied via the upstream heating network, CHP units, electrical boiler, gas boiler and HSS. Furthermore, part of the heat produced during heating market high-price periods is sold to the heating network.
- **Gas sector**: Gas load, the input of CHP units and gas boiler is fulfilled by the upstream gas network and GSS.
- **Cooling sector**: Cooling demand is provided by the ISS and absorption chiller.
- **Water sector**: Water system technologies such as SDS, WST and water well, which meet water demand by electricity consumption

3. Problem formulation

The problem formulation of the CCHPGW-MG, including the

Table 1
The comparison of reviewed literature with the current work.

Ref	Multi-energy MG			EWMG	Demand response	Objective functions			Uncertainty modelling
	CHP	CCHP	CCHPG			Energy cost	Emission cost	Water well	
(Mirzaei et al., 2020a)					✓	✓			Stochastic-Information gap decision theory
(Y. Wang et al., 2020)		✓				✓			Stochastic -robust, conditional value-at-risk (CVaR)
(Cui et al., 2020)		✓			✓	✓	✓		–
(Amir & Azimian, 2020)	✓				✓	✓	✓		Two-stage stochastic
(Mansour-Saatloo et al., 2020a)	✓				✓	✓			Robust
(Yang et al., 2020)			✓			✓			Stochastic-robust
(Ehsan & Yang, 2019)		✓				✓	✓		Scenario-based stochastic
(Moazeni & Khazaei, 2020b)				✓		✓			–
(Roustaei et al., 2020)	✓			✓		✓	✓		Scenario-based stochastic
(Zhang et al., 2020)				✓		✓	✓		–
(Sui et al., 2021)				✓		✓			–
Proposed model			✓	✓	✓	✓	✓	✓	Two-stage stochastic

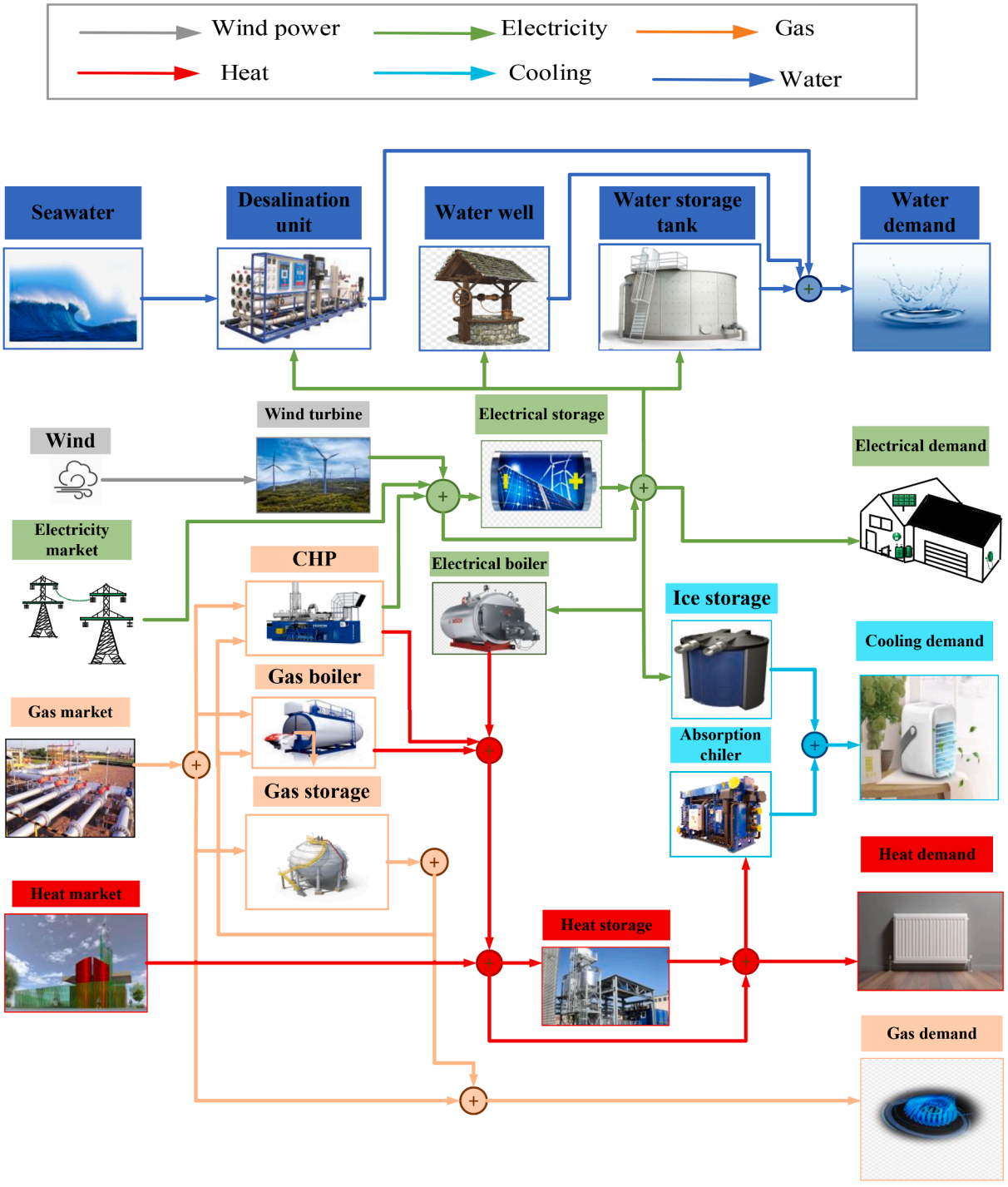

Fig. 1. Structure of the CCHPGW-MG.

objective function and constraints associated with both energy and water systems and the ε-constraint method, is given in this section.

3.1. Objective function

This paper aims to minimize the total cost, including operating and emission costs, and the amount of potable water extracted from the water well during 24 h period. The first objective is to minimize the total costs, where cost ^{O} is the operating cost and cost ^{E} is the emissions cost, as shown in Eq. (1). In Eq. (2), according to the two-stage stochastic approach in the problem, the first and second term is associated with the start-up and shut-down costs of the CHP units in the first stage, respectively. The second stage is related to the costs of operation and despatch of the integrated system that includes the third to ninth terms. The third and fourth term demonstrates cost and the revenue achieved from purchasing/selling electricity from/to the main electricity grid. The fifth and sixth term denotes cost and revenue to obtained from purchasing/selling heat from/to the main heating grid. The seventh term is associated with the cost of gas purchased from the main gas network. Finally, the eighth and ninth term is associated with the electricity DRP cost. The emissions cost is expressed using Eq. (3), in which the first, second and third terms are the carbon emission costs associated with electricity, heat, and gas purchased from the main network, respectively. The second objective is to minimize the extracted

potable water volume from the well, which is demonstrated in Eq. (4).

$$\text{Cost} = cost^{O} + cost^{E} \tag{1}$$

$$Cost^{O} = \min \sum_{j=1}^{N_j} \sum_{t=1}^{N_t} \left(C_j^{su} Y_{t,j} + C_j^{sd} Z_{t,j}\right) + \sum_{w=1}^{N_w} \rho_w \sum_{t=1}^{N_t} \begin{bmatrix} \lambda_{t,w}^{EM} P_{t,w}^{EM,imp} - \lambda_{t,w}^{EM} P_{t,w}^{EM,sell} \\ +\lambda_t^{HM} P_{t,w}^{HM,imp} - \lambda_t^{HM} P_{t,w}^{HM,sell} \\ +\lambda_t^{GM} P_{t,w}^{GM,imp} \\ +C^{EL,up} dr_{t,w}^{EL,up} + C^{EL,dn} dr_{t,w}^{EL,dn} \end{bmatrix} \tag{2}$$

$$Cost^{E} = \min \sum_{w=1}^{N_w} \rho_w \sum_{t=1}^{N_t} \left[\left(\alpha P_{t,w}^{EM,imp} + \beta P_{t,w}^{HM,imp} + \gamma P_{t,w}^{GM,imp}\right) \lambda^{C}\right] \tag{3}$$

$$Water = \min \sum_{w=1}^{N_w} \rho_w \sum_{t=1}^{N_t} \left[Q_{t,w}^{WL}\right] \tag{4}$$

3.2. CHP units constraints

Based on the essence of the cogeneration units, the heat and power generated by the CHP units are interdependent. To demonstrate this dependence, a feasible operating region (FOR) is considered for each CHP unit. In this study, the two types of CHP units the first/second type are selected with convex/non-convex FORs, respectively. Thus, each CHP unit must be operated in its FOR, which is illustrated in Fig. 2. The mathematical model and the investigation of both the types of the CHP units are taken from Hadayeghparast, Farsangi and Shayanfar (2019). Eqs. (5)-(9) are utilized to the first type of CHP unit. The presented convex FOR is modelled by the (5)-(7) equations. Besides, the limitations of the heat and power produced via the CHP unit are presented in Eqs. (8) and (9), respectively.

$$P_{t,w,j1} - P_{j1}^{A} - \frac{P_{j1}^{A} - P_{j1}^{B}}{H_{j1}^{A} - H_{j1}^{B}} \times \left(H_{t,w,j1} - H_{j1}^{A}\right) \le 0 \tag{5}$$

$$P_{t,w,j1} - P_{j1}^{B} - \frac{P_{j1}^{B} - P_{j1}^{C}}{H_{j1}^{B} - H_{j1}^{C}} \times \left(H_{t,w,j1} - H_{j1}^{B}\right) \ge -\left(1 - I_{t,j}\right) \times K \tag{6}$$

$$P_{t,w,j1} - P_{j1}^{C} - \frac{P_{j1}^{C} - P_{j1}^{D}}{H_{j1}^{C} - H_{j1}^{D}} \times \left(H_{t,w,j1} - H_{j1}^{C}\right) \ge -\left(1 - I_{t,j}\right) \times K \tag{7}$$

$$0 \le H_{t,w,j1} \le H_{j1}^{B} \times I_{t,j} \tag{8}$$

$$0 \le P_{t,w,j1} \le P_{j1}^{A} \times I_{t,j} \tag{9}$$

Eqs. (10)-(18) are used for the second type of CHP unit. Since the second type CHP has a non-convex FOR, its formulation is different from the first type CHP with convex FOR. Hence, in the formulation structure of the second type CHP, two binary variables $V_{1,t}$and $V_{2,t}$are utilized. Therefore, the non-convex FOR is divided into two convex subsections (a) and (b), as demonstrated in Fig. 2. The presented FOR for the second type CHP is modelled by the (10)-(13) equations. Eqs. (14) and (15) represent the maximum of the heat and power produced by the CHP unit, respectively. In Eqs. (16)-(18), the binary variables $V_{1,t}$and $V_{2,t}$ are utilized to determine the sector where the operating point of the CHP unit is located. Eq. (16) illustrates, which when the CHP unit is ON, the operating sector of this unit would be either (a) [$V_{1,t}$= 1, $V_{2,t}$= 0] or (b) [$V_{1,t}$= 0, $V_{2,t}$= 1].

$$P_{t,w,j2} - P_{j2}^{B} - \frac{P_{j2}^{B} - P_{j2}^{C}}{H_{j2}^{B} - H_{j2}^{C}} \times \left(H_{t,w,j2} - H_{j2}^{B}\right) \le 0 \tag{10}$$

$$P_{t,w,j2} - P_{j2}^{C} - \frac{P_{j2}^{C} - P_{j2}^{D}}{H_{j2}^{C} - H_{j2}^{D}} \times \left(H_{t,w,j2} - H_{j2}^{C}\right) \ge 0 \tag{11}$$

$$P_{t,w,j2} - P_{j2}^{E} - \frac{P_{j2}^{E} - P_{j2}^{F}}{H_{j2}^{E} - H_{j2}^{F}} \times \left(H_{t,w,j2} - H_{j2}^{E}\right) \ge -\left(1 - V_{1,t}\right) \times K \tag{12}$$

$$P_{t,w,j2} - P_{j2}^{D} - \frac{P_{j2}^{D} - P_{j2}^{E}}{H_{j2}^{D} - H_{j2}^{E}} \times \left(H_{t,w,j2} - H_{j2}^{D}\right) \ge -\left(1 - V_{2,t}\right) \times K \tag{13}$$

$$0 \le P_{t,w,j2} \le P_{j2}^{A} \times I_{t,j} \tag{14}$$

$$0 \le H_{t,w,j2} \le H_{j2}^{C} \times I_{t,j} \tag{15}$$

$$V_{1,t} + V_{2,t} = I_{t,j} \tag{16}$$

$$H_{t,w,j2} - H_{j2}^{E} \le \left(1 - V_{1,t}\right) \times K \tag{17}$$

$$H_{t,w,j2} - H_{j2}^{E} \ge -\left(1 - V_{2,t}\right) \times K \tag{18}$$

Eq. (19) expresses the relation between the binary variables of CHP units. Eqs. (20)-(21) illustrate the minimum on/off time constraints of the CHP units, respectively (Zhou et al., 2019).

$$I_{t,j} - I_{t-1,j} = Y_{t,j} - Z_{t,j} \tag{19}$$

$$I_{\tau,j} \ge Y_{t,j} \qquad \forall t \le \tau \le t + T_j^{ON} - 1 \tag{20}$$

$$1 - I_{\tau,j} \ge Z_{t,j} \quad \forall t \le \tau \le t + T_j^{OFF} - 1 \tag{21}$$

Eq. (22) demonstrates the value of gas consumed via CHP units (Mirzaei et al., 2020b).

$$GC_{t,w,j} = \frac{P_{t,w,j}}{\eta_j} + SU_{t,j} + SD_{t,j} \tag{22}$$

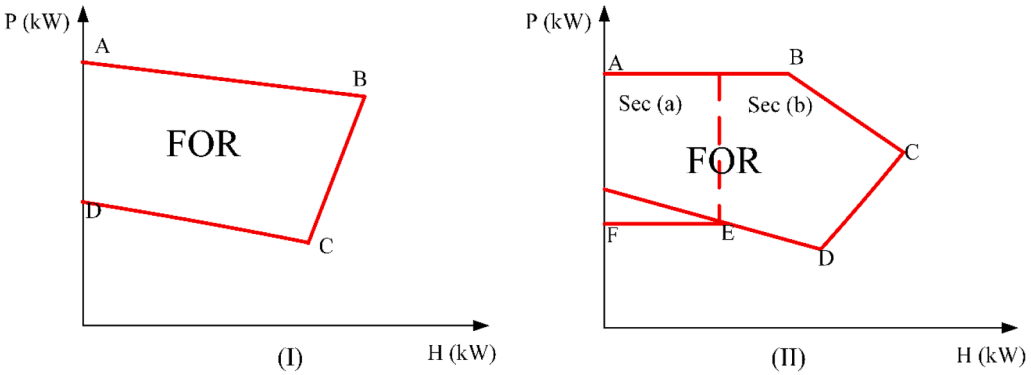

Fig. 2. FOR for CHP units (I) first type, (II) second type.

3.3. Gas boiler constraints

A gas boiler (GB) is a device, which produces heat via natural gas. The value of gas utilized by the GB and the heat produced by it are expressed in Eq. (23). Also, the amount of maximum and minimum heat produced by the GB is defined by Eq. (24) (Mansour-Saatloo et al., 2020b).

$$GB_{t,w}^{gb} = \frac{H_{t,w}^{gb}}{\eta^{gb}} \tag{23}$$

$$H^{gb,\min} \times I_{t,w}^{gb} \le H_{t,w}^{gb} \le H^{gb,\max} \times I_{t,w}^{gb} \tag{24}$$

3.4. Electric boiler constraints

The electric boiler (EB) generates heat by consuming electricity. The amount of electricity consumed via the EB and the heat produced by it is demonstrated in Eq. (25). Also, the amount of maximum and minimum heat produced by the EB is calculated by Eq. (26) (Nasiri et al., 2020).

$$EB_{t,w}^{eb} = \frac{H_{t,w}^{eb}}{\eta^{eb}} \tag{25}$$

$$H^{eb,\min} \times I_{t,w}^{eb} \le H_{t,w}^{eb} \le H^{eb,\max} \times I_{t,w}^{eb} \tag{26}$$

3.5. Heat storage system constraints

The stored heat in the HSS is determined by Eq. (27). According to Eq. (28), the reserved heat is limited between the minimum and maximum reservoir capacity. Furthermore, the limitations of charge and discharge modes are demonstrated in Eqs. (29) and (30), respectively. Finally, Eq. (31) states which the HSS cannot be charged and discharged, simultaneously (Mansour-Saatloo et al., 2020a).

$$E_{t,w}^{HS} = \left(1-\eta^{HS}\right)E_{t-1,w}^{HS} + \eta^{HS,ch}H_{t,w}^{HS,ch} - \frac{H_{t,w}^{HS,disch}}{\eta^{HS,disch}} \tag{27}$$

$$E^{HS,\min} \le E_{t,w}^{HS} \le E^{HS,\max} \tag{28}$$

$$E_{t,w}^{HS} - E_{t-1,w}^{HS} \le E^{HS,ch,\max} \tag{29}$$

$$E_{t-1,w}^{HS} - E_{t,w}^{HS} \le E^{HS,disch,\max} \tag{30}$$

$$I_{t,w}^{HS,ch} + I_{t,w}^{HS,disch} \le 1 \tag{31}$$

3.6. Gas storage system constraints

The value of reserved gas in the GSS is expressed in Eq. (32) and is limited via Eq. (33). In addition, the GSS charge and discharge modes are limited via Eqs. (34) and (35), respectively. Eq. (36) prevents the simultaneous charge and discharge of the GSS (Mansour-Saatloo et al., 2020a).

$$E_{t,w}^{GS} = E_{t-1,w}^{GS} + \left(\eta^{ch,GS} \times P_{t,w}^{ch,GS} - \frac{P_{t,w}^{disch,GS}}{\eta^{disch,GS}}\right) \times \Delta t \tag{32}$$

$$E^{GS,\min} \le E_{t,w}^{GS} \le E^{GS,\max} \tag{33}$$

$$P^{ch,GS,\min} I_{t,w}^{ch,GS} \le P_{t,w}^{ch,GS} \le P^{ch,GS,\max} I_{t,w}^{ch,GS} \tag{34}$$

$$P^{disch,GS,\min} I_{t,w}^{disch,GS} \le P_{t,w}^{disch,GS} \le P^{disch,GS,\max} I_{t,w}^{disch,GS} \tag{35}$$

$$I_{t,w}^{ch,GS} + I_{t,w}^{disch,GS} \le 1 \tag{36}$$

3.7. Electrical storage system constraints

The value of reserved electrical in the ESS is showed in Eq. (37) and is limited in Eq. (38). Furthermore, ESS charging/discharging modes are limited via Eqs. (39) and (40), respectively. Finally, Eq. (41) prevents the ESS charge and discharge simultaneously. (Mansour-Saatloo et al., 2020a).

$$E_{t,w}^{ES} = E_{t-1,w}^{ES} + \left(\eta^{ch,ES} \times P_{t,w}^{ch,ES} - \frac{P_{t,w}^{disch,ES}}{\eta^{disch,ES}}\right) \times \Delta t \tag{37}$$

$$E^{ES,\min} \le E_{t,w}^{ES} \le E^{ES,\max} \tag{38}$$

$$P^{ch,ES,\min} I_{t,w}^{ch,ES} \le P_{t,w}^{ch,ES} \le P^{ch,ES,\max} I_{t,w}^{ch,ES} \tag{39}$$

$$P^{disch,ES,\min} I_{t,w}^{disch,ES} \le P_{t,w}^{disch,ES} \le P^{disch,ES,\max} I_{t,w}^{disch,ES} \tag{40}$$

$$I_{t,w}^{ch,ES} + I_{t,w}^{disch,ES} \le 1 \tag{41}$$

3.8. Ice storage system constraints

The ISS is a type of storage system, which can meet the cooling demand by consuming electricity. The ISS level is presented in Eq. (42) and is limited by Eq. (43). Also, the limitations of charge and discharge modes are expressed in Eqs. (44) and (45), respectively. Eq. (46) expresses that the ISS cannot be charged and discharged simultaneously. (Mansour-Saatloo et al., 2020b).

$$E_{t,w}^{ISS} = E_{t-1,w}^{ISS} + \left(\eta^{ch,ISS} \times P_{t,w}^{ch,ISS} - \frac{P_{t,w}^{disch,ISS}}{\eta^{disch,ISS}}\right) \times \Delta t \tag{42}$$

$$E^{ISS,\min} \le E_{t,w}^{ISS} \le E^{ISS,\max} \tag{43}$$

$$P^{ch,ISS,\min} I_{t,w}^{ch,ISS} \le P_{t,w}^{ch,ISS} \le P^{ch,ISS,\max} I_{t,w}^{ch,ISS} \tag{44}$$

$$P^{disch,ISS,\min} I_{t,w}^{disch,ISS} \le P_{t,w}^{disch,ISS} \le P^{disch,ISS,\max} I_{t,w}^{disch,ISS} \tag{45}$$

$$I_{t,w}^{ch,ISS} + I_{t,w}^{disch,ISS} \le 1 \tag{46}$$

3.9. Absorption chiller

The absorption chiller is a device which by using thermal energy to provide the cooling demand. Eq. (47) demonstrates the value of generated cooling energy through the absorption chiller, which is limited in Eq. (48) (Mansour-Saatloo et al., 2020b).

$$C_{t,w}^{abchlr} = H_{t,w}^{abchlr} \times \eta^{abchlr} \tag{47}$$

$$C^{abchlr,\min} \le C_{t,w}^{abchlr} \le C^{abchlr,\max} \tag{48}$$

3.10. Electrical demand response

Electrical DRP is one of the efficient methods to handle electrical demands. Accordingly, electrical demands are shifted from peak hours to off-peak hours. Eqs. (49) and (50) represents the limitation of shiftable electrical demands. Eq. (51) illustrate total shifted demands should be equal to total curtailed demands. Therefore, after applying electrical DRP, total electrical demand is given via Eq. (52) (Mansour-Saatloo et al., 2020b).

$$0 \le dr_{t,w}^{EL,up} \le DRE \times ED_{t,w} \tag{49}$$

$$0 \le dr_{t,w}^{EL,dn} \le DRE \times ED_{t,w} \tag{50}$$

$$\sum_{t=1}^{N_t} dr_{t,w}^{EL,up} = \sum_{t=1}^{N_t} dr_{t,w}^{EL,dn} \tag{51}$$

$$ED_{t,w}^{DR} = ED_{t,w} + dr_{t,w}^{EL,up} - dr_{t,w}^{EL,dn} \tag{52}$$

3.11. Water system model

The formulation of the water system expresses in this section, which includes several components such as SDS, WST and water well. In this study is assumed which the WST pump consumes electricity when it is in charge mode and the water well pump uses electricity when water is extracted from it, as well as the water level in the well is assumed to be constant due to the short-time optimization period (Pakdel et al., 2020). Eq. (53) is the water balance constraint, which expresses that the obtained water from the SDS, WST and water well must be equal to the total water demand.

$$Q_{t,w}^{WL} + Q_{t,w}^{D} - Q_{t,w}^{S,ch} + Q_{t,w}^{S,disch} = WD_t \tag{53}$$

Water is pumped into the WST via the water source, such as a well or any other source, and the WST holds clean and excess water to meet the water demand for periods of low water. Eq. (54) represents the water level in WST and limits by Eq. (55). Eqs. (56) and (57) shows the limitation of charge and discharge of the WST. Finally, Eq. (58) prevents simultaneous occurrence of charging and discharging of the WST (Pakdel et al., 2020).

$$LS_{t,w} = LS_{t-1,w} + \frac{Q_{t,w}^{S,ch}}{CS} - \frac{Q_{t,w}^{S,disch}}{CS} \tag{54}$$

$$0 \le LS_{t,w} \le LS^{\max} \tag{55}$$

$$Q_{t,w}^{S,ch} \le Q^{S,ch,\max} I_{t,w}^{S,ch} \tag{56}$$

$$Q_{t,w}^{S,disch} \le Q^{S,disch,\max} I_{t,w}^{S,disch} \tag{57}$$

$$0 \le I_{t,w}^{S,ch} + I_{t,w}^{S,disch} \le 1 \tag{58}$$

Eqs. (59) and (60) show the power consumption by the water well pump and the WST pump at time t and scenario w, respectively. Also, 3.6×10^6 in the denominator of Eqs. (59) and (60) is utilized to convert used power in the W range within 1 second to power consumption in the kW range during a 1hour period (Pakdel et al., 2020).

$$P_{t,w}^{PWL} = Q_{t,w}^{WL} L^{WL} \frac{g\varphi}{\eta^{PWL}\left(3.6 \times 10^6\right)} \tag{59}$$

$$P_{t,w}^{PS} = Q_{t,w}^{S,ch}\left(LS_{t,w} + LS_{t-1,w} + L^{G}\right) \frac{g\varphi}{2\eta^{PS}\left(3.6 \times 10^6\right)} \tag{60}$$

The SDS consumes an abundance of energy in comparison with conventional water treatment methods. In particular, energy consumption for typical water treatment methods is around 0.06 kWh/m^3, while the SDS energy consumption is altering between 0.5–16 kWh/m^3, depending on the type of the SDS. The SDS technologies are chiefly categorized into two types of membrane processes and thermal processes. Thermal processes utilize thermal and electrical energy for desalination, in which the required thermal and electrical energy between 4 and 12 kWh/m^3 and 1.5–4 kWh/m^3 is fluctuating, respectively. Membrane processes utilize only electrical energy for desalination and their required energy between 0.5–4 kWh/m^3 is altering. Membrane processes use lower energy than thermal processes due to the prevention of seawater evaporation. The reverse osmosis (RO) is a kind of membrane process that is considered a superior desalination technology due to the less energy usage, lower costs, and technological developments (Caldera, Bogdanov & Breyer, 2016; Pakdel et al., 2020). Accordingly, the RO membrane process is considered as the desalination unit in this work. The amount of power consumed by SDS to remove salt from seawater and meet the potable water demand is expressed via Eq. (61), and water obtained from SDS is limited by Eq. (62) (Pakdel et al., 2020).

$$P_{t,w}^{D} = \eta^{D} Q_{t,w}^{D} \tag{61}$$

$$0 \le Q_{t,w}^{D} \le Q^{D,\max} \tag{62}$$

As mentioned above, there are diverse methods for seawater desalination. In this study, the seawater salinity 35 PSU (Practical Salinity Unit) is supposed. Accordingly, the energy efficiency of the SDS 3.0348 kWh/m^3 is calculated (Caldera et al., 2016; Pakdel et al., 2020).

Total power consumption by water network consists of power consumed by the SDS, water well pump and WST pump as Eq. (63).

$$P_{t,w}^{water} = P_{t,w}^{D} + P_{t,w}^{PWL} + P_{t,w}^{PS} \tag{63}$$

3.12. Multi-energy balance constraints

According to Eq. (64), the electricity demand and power required by the water network, electric boiler, ISS charging, ESS charging and electricity sold to the main grid can be met via the electricity bought from the main network and power produced by the first and second type CHP units, wind turbine and ESS discharging. The gas imported from the main grid and GSS discharging, are provided the gas demand and gas needed for equipment such as first and second type CHP units, gas boiler and GSS charging, which is calculated by Eq. (65). The heat demand, the input heat of absorption chiller, HSS charging and heat sold to the main grid, must be provided by purchasing heat from the main network and heat generated by the first and second type CHP units, HSS discharging, electric boiler and gas boiler that is shown in Eq. (66). Eq. (67) expresses that the cooling demand is supplied via the ISS discharging and absorption chiller.

$$P_{t,w}^{EM,imp} - P_{t,w}^{EM,sell} + P_{t,w}^{wind} - P_{t,w}^{ch,ES} + P_{t,w}^{disch,ES} - EB_{t,w}^{eb} - P_{t,w}^{ch,ISS} - P_{t,w}^{Water} + \sum_{j=1}^{N_j} P_{t,w,j} = ED_{t,w}^{DR} \tag{64}$$

$$P_{t,w}^{GM,imp} - P_{t,w}^{ch,GS} + P_{t,w}^{disch,GS} - GB_{t,w}^{gb} - \sum_{j=1}^{N_j} GC_{t,w,j} = GD_t \tag{65}$$

$$P_{t,w}^{HM,imp} - P_{t,w}^{HM,sell} + H_{t,w}^{HS,disch} - H_{t,w}^{HS,ch} + H_{t,w}^{gb} + H_{t,w}^{eb} - H_{t,w}^{abchlr} + \sum_{j=1}^{N_j} H_{t,w,j} = HD_t \tag{66}$$

$$C_{t,w}^{abchlr} + P_{t,w}^{disch,ISS} = CD_t \tag{67}$$

3.13. Multi-objective problem optimization

3.13.1. The ε-constraint method

In multi-objective problems, there is more than one objective, in which objective functions are entirely conflicting, and all objectives cannot be optimized simultaneously. Hence, decision-makers are looking to find the best solution. A technique to solve multi-objective problems is using the ε-constraint method, which is a practical solution for solving multi-objective problems with conflicting objective functions. Moreover, a multi-objective optimization problem like Eq. (68) with k objectives could be solved utilizing the ε-constraint method (Nazari-Heris, Mirzaei, Mohammadi-Ivatloo, Marzband & Asadi, 2020).

$$\begin{aligned} &\max \quad (f_1(x), f_2(x), \ldots, f_k(x)) \\ &S.t. \\ &x \in R \end{aligned} \tag{68}$$

Where, x and R represent the decision variables and feasible region,

respectively. Accordingly, the multi-objective problem is solved by considering each objective function separately and converts to a single-objective problem. Thus, one of the objectives is considered as the main objective function so that this main objective function is optimized, while other objectives as constraints are considered, which is as follows:

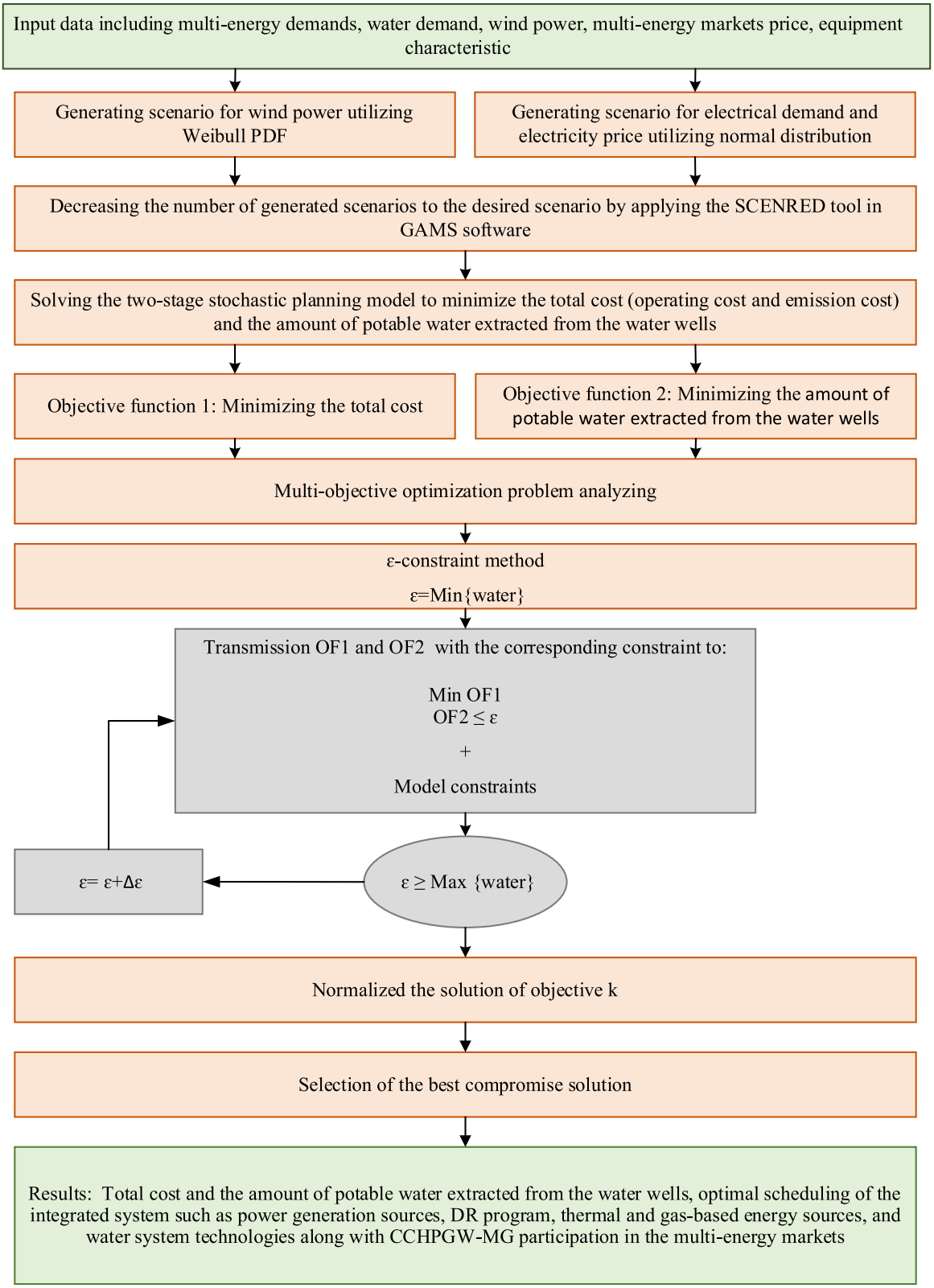

Fig. 3. Flowchart of the whole problem optimization process.

$$\begin{aligned} &\max \quad f_1(x) \\ &S.t. \\ &\quad f_2(x) \geq \varepsilon_2, \\ &\quad f_3(x) \geq \varepsilon_3, \\ &\quad \ldots \\ &\quad f_k(x) \geq \varepsilon_k, \\ &\quad x \in R \end{aligned} \tag{69}$$

In this study, the objective function associated with cost (including operation and emission costs) as the main objective function and objective function associated with the value of potable water extracted from the well as a constraint is considered. To obtain the optimal solution to the problem, the parameters of the ε-constraint method $(\varepsilon_2, \varepsilon_3, \ldots, \varepsilon_k)$ are changed parametrically. The values $(\varepsilon_2, \varepsilon_3, \ldots, \varepsilon_k)$ are based on the range of the k-1 objective functions.

3.13.2. Fuzzy approach

After solving a multi-objective problem, the set of optimal solutions called the Pareto front is obtained, while only one optimal solution using the fuzzy approach can be selected, which is expressed as the best compromise solution. The fuzzy method assigns a fuzzy membership value in [0, 1] for each solution obtained in the Pareto front. The fuzzy membership function for the objective functions of this problem can be calculated as follows (Nazari-Heris, Abapour & Mohammadi-Ivatloo, 2017):

$$\widehat{f}_k = \begin{cases} 1 & f_k < f_k^{\min} \\ \dfrac{f_k^{\max} - f_k}{f_k^{\max} - f_k^{\min}} & f_k^{\min} < f_k < f_k^{\max} \\ 0 & f_k > f_k^{\max} \end{cases} \tag{70}$$

The best compromise solution by using the min-max technique is obtained. According to this technique, the minimum value of f_1 and f_2 is provided, and then choosing the best compromise solution as the maximum amount of min $(\widehat{f}_1, \widehat{f}_2)$. Fig. 3 demonstrates of the whole problem optimization process.

4. Simulation and numerical results

4.1. Input data

The proposed model is utilized for day-ahead scheduling of the CCHPGW-MG, as demonstrated in Fig. 1. Further, the comprehensive information on CCHPGW-MG technologies and carbon emissions is given in Table 2 (Agabalaye-Rahvar, Mansour-Saatloo, Mirzaei, Mohammadi-Ivatloo & Zare, 2021; Mansour-Saatloo et al., 2020a, 2020b; Pakdel et al., 2020). In addition, the FOR characteristics of the first and second-type CHP units are presented in Table 3 (Hadayeghparast et al., 2019). The microgrid operator is supplied via upstream

Table 2
Data of the CCHPGW-MG technologies.

	Parameter	Unit	Value		Parameter	Unit	Value
CHP units0	T_j^{ON}	h	2	**Ice storage**	$\eta^{ch,ISS}$	–	0.96
	T_j^{OFF}	h	2		$\eta^{disch,ISS}$	–	0.96
	η_{j1}	–	0.3		$E^{ISS,\max}$	kWh	200
	η_{j2}	–	0.35		$E^{ISS,\min}$	kWh	5
Gas boiler	η^{gb}	–	0.9		$P^{ch,ISS,\max}$	kW	50
	$H^{gb,\max}$	kW	80		$P^{ch,ISS,\min}$	kW	5
	$H^{gb,\min}$	kW	15		$P^{disch,ISS,\max}$	kW	50
Electrical boiler	η^{eb}	–	2		$P^{disch,ISS,\min}$	kW	5
	$H^{eb,\max}$	kW	40	**Absorption chiller**	η^{abchlr}	–	0.75
	$H^{eb,\min}$	kW	5		$C^{abchlr,\max}$	kW	70
Heat storage	η^{HS}	–	0.05		$C^{abchlr,\min}$	kW	10
	$\eta^{HS,ch}$	–	0.9	**Demand response**	DRE	%	10
	$\eta^{HS,disch}$	–	0.9		$C^{EL,up}$	$/kWh	0.0025
	$E^{HS,\max}$	kWh	750		$C^{EL,dn}$	$/kWh	0.0025
	$E^{HS,\min}$	kWh	0	**Carbon emission**	λ^C	$/kg	0.02
	$E^{HS,ch,\max}$	kW	150		α	kg/kWh	0.92125
	$E^{HS,disch,\max}$	kW	150		β	kg/kWh	0.56267
Gas storage	$\eta^{ch,GS}$	–	0.95		γ	kg/kWh	0.2764
	$\eta^{disch,GS}$	–	0.95	**Water**	CS	m^2	4
	$E^{GS,\max}$	kWh	800		$LS^{\max}$	m	39.2
	$E^{GS,\min}$	kWh	0		$Q^{S,ch,\max}$	m^3/h	28
	$P^{ch,GS,\max}$	kW	200		$Q^{S,disch,\max}$	m^3/h	28
	$P^{ch,GS,\min}$	kW	20		L^{WL}	m	10
	$P^{disch,GS,\max}$	kW	200		g	m/s^2	9.81
	$P^{disch,GS,\min}$	kW	20		φ	kg/m^3	1000
Electrical storage	$\eta^{ch,ES}$	–	0.95		η^{PWL}	–	0.85
	$\eta^{disch,ES}$	–	0.95		η^{PS}	–	0.85
	$E^{ES,\max}$	kWh	600		η^{D}	kWh/m^3	3.0348
	$E^{ES,\min}$	kWh	60		L^G	m	4
	$P^{ch,ES,\max}$	kW	100		$Q^{D,\max}$	m^3/h	40
	$P^{ch,ES,\min}$	kW	20		LS_0	m	2
	$P^{disch,ES,\max}$	kW	100				
	$P^{disch,ES,\min}$	kW	20				

Table 3
FOR characteristics of CHP units.

The first type of CHP		The second type of CHP	
A (P, H)	(120, 0)	A (P, H)	(125.8, 0)
B (P, H)	(105, 87.5)	B (P, H)	(125.8, 32.4)
C (P, H)	(40, 50.9)	C (P, H)	(110.2, 135.6)
D (P, H)	(48, 0)	D (P, H)	(40, 75)
		E (P, H)	(44, 15.9)
		F (P, H)	(44, 0)

electricity, gas and heating networks, wind turbines and water. The forecasted prices for the electricity, heat and gas markets are shown in Fig. 4 (Mansour-Saatloo et al., 2020a; Murillo-Sánchez, Zimmerman, Anderson & Thomas, 2013; Oskouei et al., 2021). Furthermore, Fig. 5 illustrates the different demands, i.e., electricity, heat, cooling, gas and power generated through wind turbine (Mansour-Saatloo et al., 2020a; Mirzaei, Zare, Mohammadi-Ivatloo, Marzband & Anvari-Moghaddam, 2021), and Fig. 6 presents the water demand (Pakdel et al., 2020).

As mentioned before, to handle the uncertainties related to the electrical demand, wind power, and electricity market price was adopted a two-stage stochastic approach in this work. Weibull PDF has been utilized in numerous research papers for modelling wind power uncertainty because of its high adaptability (Mansour-Saatloo et al., 2020b). Accordingly, the Weibull PDF is used to model wind power uncertainty, and the normal distribution is utilized to model electrical demand and electricity price uncertainties in this study. Furthermore, to simulate the aforementioned uncertainties, 1000 scenarios are generated utilizing the Monte Carlo simulation technique. However, due to the computational complexity of a large number of scenarios, the produced scenarios are decreased to 10 by the SCENRED tool in GAMS software. The SCENRED tool in GAMS software contains two scenario reduction approaches such as fast-forward approach and fast-backward approach. Specifically, the fast-backward approach is faster than the fast-forward approach in terms of computational time, but the achieved results of the forward approach are more accurate than the backward approach so that the fast-forward approach needs more computational time (Mirzaei et al., 2021). SCENRED is capable of selecting the desired number of preserved scenarios, named as Red_num_leaves. Further, the red_percentage is an option of SCENRED that operates according to the relative distance between the initial and decreased scenarios (Jalilian, Mansour-Saatloo, Mirzaei, Mohammadi-Ivatloo & Zare, 2021). In this study, a fast-backward scenario reduction algorithm is applied with the Red_num_leaves factor of 10 to minimize the computational complexity, the computational time and enhance the performance accuracy.

In this work, a mixed-integer non-linear programming (MINLP) problem is solved utilizing DICOPT solver in GAMS software that the nonlinearity of the problem is due to the equations of the WST pump, in which the number of single variables is 13,474 and the number of single equations is 19,582. The optca and optcr options of the DICOPT solver to solve the MINLP problem are set as optca=0.0 and optcr=0.0. In fact, Optca option represents an absolute termination toleration for a solver of the global. when the absolute gap from optca option is not high, the solver stops. Optcr option specifies a relative termination toleration for a solver of the global. After evaluating an optimal solution that is in the range of specified toleration with optcr, the solver stops and therefore the time of the solution may be decreased (Mirzaei et al., 2020a). Since the options optca=0.0 and optcr=0.0, it is concluded that the optimality loss in this problem is zero. GAMS is an optimization software to model mathematical problems and to solve nonconvex and convex problems. Results gained from DICOPT solver can be provided a set of global optimality solutions to a reliable extent, which has been discussed in previous works (Ahrabi et al., 2021; Mirzaei et al., 2020a; Moazeni & Khazaei, 2020a, b; Moazeni et al., 2020; Pakdel et al., 2020). DICOPT solver solves an MINLP problem using the sub-problems of NLP and MIP, which NLP sub-problem solves through CONOPT solver and MIP sub-problem solves through CPLEX solver. Fig. 7 illustrates the Flowchart of DICOPT solver to solve MINLP problem.

4.2. Results

The optimal scheduling of water-energy sources of the proposed model is investigated under system uncertainties in three subsections.

4.2.1. The optimal scheduling of power-based sources and DR program along with CCHPGW-MG participation in the power market

A multi-objective optimization problem is solved by considering uncertainties associated with electrical demand, wind power and electricity price under a two-stage stochastic approach to minimize the total cost (operating and emission costs) and amount of potable water extracted from water wells, simultaneously. Fig. 8 shows the CCHPGW-MG Pareto optimal solutions using the ε-constraint method. Based on this figure, by increasing cost, the volume of water extracted from the well decreases. This means that from the point of view of the water objective function, to minimize the volume of water extracted from the well, the SDS must be used as much as possible to provide the water demand without extracting water from the well, which this subject increases the cost of operation, due to the SDS consumes the significant amount of energy. In addition, from the point of view of the cost

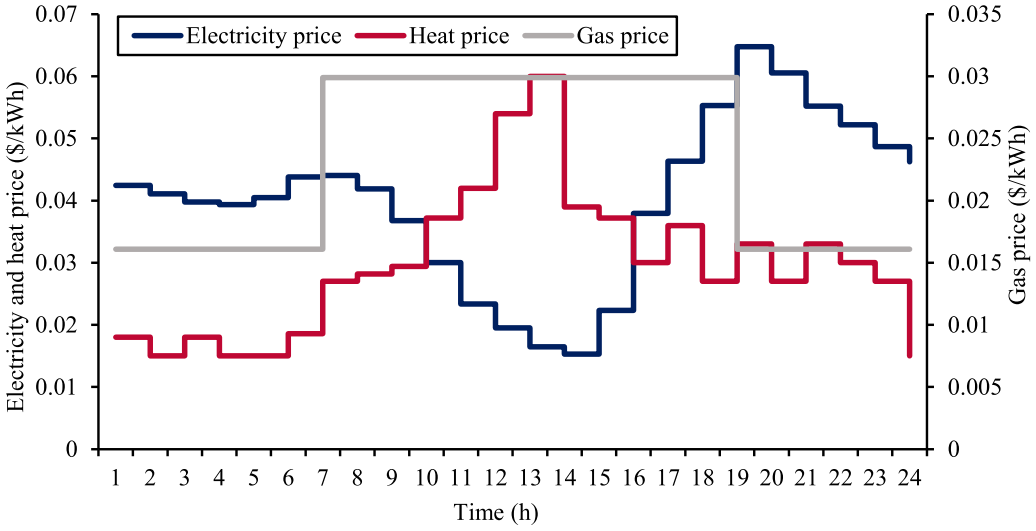

Fig. 4. Forecasted electricity, heat and gas market prices.

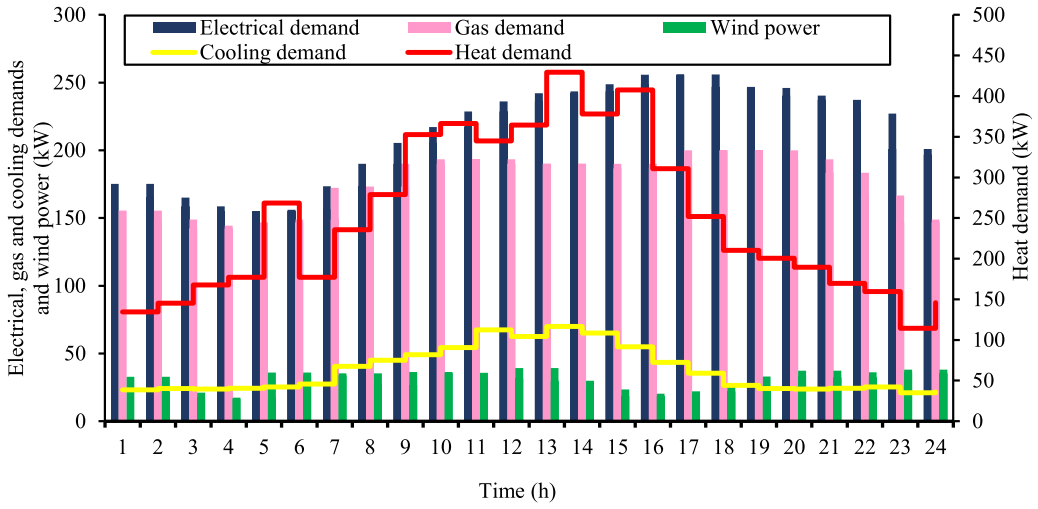

Fig. 5. Wind power and demands.

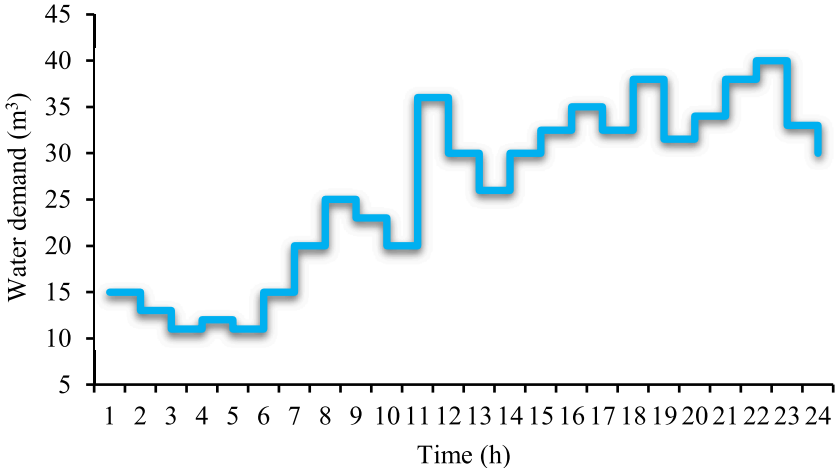

Fig. 6. Water demand.

objective function, the water demand must be met via water extracted from the well without utilizing the SDS to minimize total cost. With respect to the value of fuzzy membership function in [0, 1], the production of Pareto optimal solutions with steps of 0.05 is proposed in this study, and 21 iterations are considered to generate Pareto optimal solutions. As discussed before, the fuzzy approach is utilized to determine the best compromise solution. Based on Fig. 8, the optimal solution is achieved in the 16th iteration, where the value of the maximum weakest membership function in the 16th iteration equal to 0.750. According to the results of this iteration, the total cost and the value of water extracted for the optimal solution equal to \$592.248 and 157.875 m^3, respectively.

Fig. 9 presents the electrical power supply and demand balance per hour. The expected optimal values of power above the horizontal axis/ below the horizontal axis illustrate the electrical power generation/ electrical power consumption. As seen in Fig. 9, the CCHPGW-MG operator buys power from the market as a consumer in hours when the electricity price is low (10 to 15) and sells power to the market as a seller in hours when high electricity price (19 to 21), thus reducing costs. During off-peak electricity price hours, CHP units reduce their output power generation because purchase power from the market is more cost-effective than power generation via CHP units. However, at peak electricity price hours, these units increase their output power generation and provide part of the electrical load. In addition, wind power meets part of the electrical load at all hours. The ESS is operated at electricity market price off-peak hours (10 to 15) in the charging mode, then at electricity market price peak hours (18 to 22) is operated in the discharging mode. The water network consumes power at all hours to meet the required water demand, but as demonstrated in Fig. 9, the amount of power consumed via the water network during off-peak hours of electricity price is higher than peak hours of electricity price. The ISS also consumes power, during off-peak hours of electricity price to supply cooling demand, in other words, in this state the ISS is operated in charging state. Furthermore, due to the dependence of the electric boiler on the market price of heat and electricity, it is more economical (for example, between $t = 6$ and $t = 19$) to participate in the electricity market. The impact of the ESS and DRP on power trading with the market is illustrated in Fig. 10. As obvious in this figure, due to the presence of ESS and DR, the value of power sold to market during peak hours of electricity price (19 to 21) and the purchased power from the market during off-peak hours of electricity price (10 to 15) significantly has increased. Also, the effect of ESS is much rather than the DR program. Fig. 11 represents the variation of electrical demand by applying the DR program. Based on this figure, the electrical demand is shifted from electricity price peak hours (18 to 23) to electricity price off-peak hours (10 to 15).

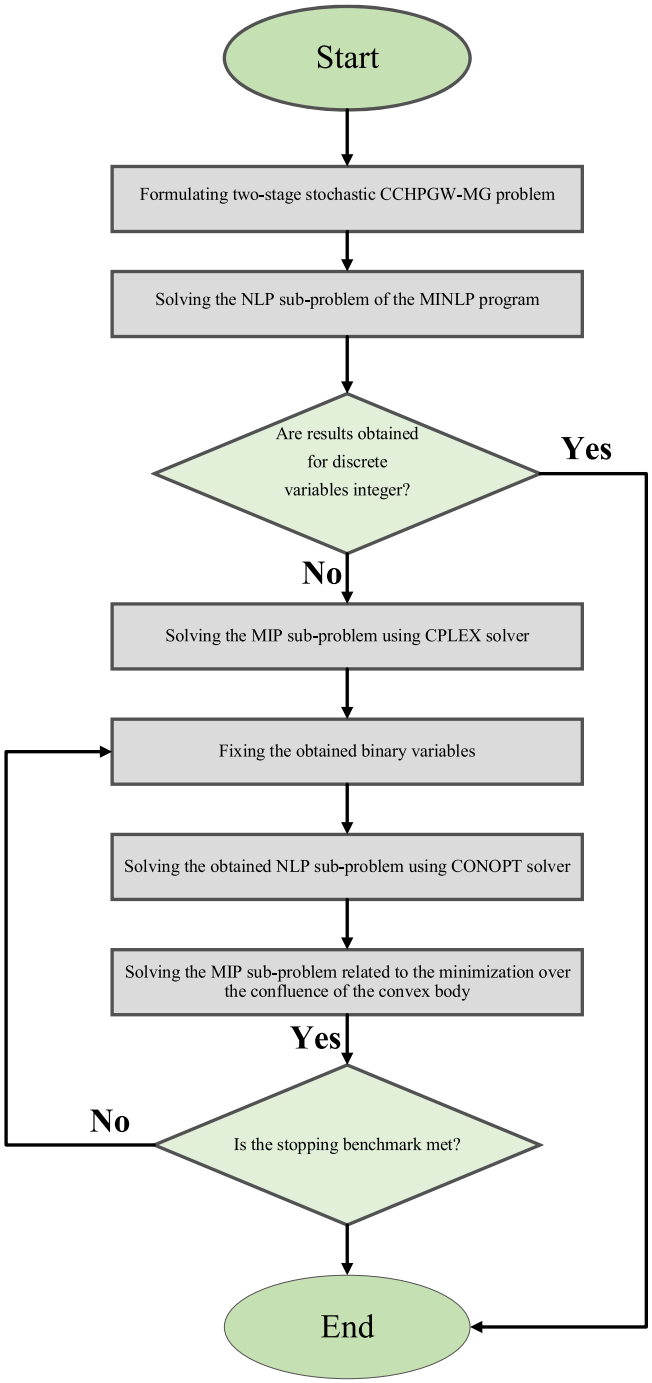

Fig. 7. Flowchart of DICOPT solver to solve MINLP program.

4.2.2. The optimal scheduling of thermal and gas-based energy sources along with CCHPGW-MG participation in the heat, gas and power market

In this section, according to the optimal solution achieved from solving the multi-objective optimization problem in the previous section, the optimal scheduling of the thermal and gas-based energy sources is investigated. The heating power supply and demand balance demonstrate in Fig. 12. The expected optimal values of heat above and below the horizontal axis illustrate the generation and consumption of the heat, respectively. It can be obvious in this figure that a significant part of the heat load is provided via CHP units. As mentioned earlier, due to the electrical boiler's dependence on the market price of heat and electricity, it is more economical for this unit (for example, between t = 6 and t = 19) to generate heat.

The gas boiler is also applied in most hours to supply the heat demand at its maximum capacity. The HSS dependant on the heat market price and heat generation by the CHP units, so in hours when the heat market price is low and the value of heat produced via CHP units is high (t = 1–6 and t = 23–24) is operated in the charge state, and then during the hours when the market price of heat is high and the value of heat produced via the CHP units is low (10 to 13) is operated in the discharge mode. Furthermore, the CCHPGW-MG operator buys heat from the market as a consumer in hours when the value of heat produced via the CHP units is low (t = 7–11 and t = 13–18) and then sell the heat to the market as a seller in hours when the value of heat produced via the CHP units is high (19 to 23). The absorption chiller also uses heat at all hours to provide the cooling demand. Fig. 13 shows the gas supply and demand balance. The expected optimal values of gas above and below the horizontal axis demonstrate the generation and consumption of the gas, respectively. Based on this figure, CHP units consumes gas at all hours to provide heat and power load, so that the amount of gas consumed via CHP units during gas price peak hours (7 to 18) is much less the amount of gas consumed during gas price off-peak hours (t = 1–6 and t = 19–24). Also, the CCHPGW-MG operator prefers to buy less gas from the market during peak gas price hours. Due to the dependence of GSS on the price of the gas market is operated in the charging state at gas price off-peak hours (t = 2,4,5,6 and t = 22–24) and then is operated in the discharging state at gas price peak hours (7 to 11). In addition, due to the low price of the gas market, the gas boiler also consumes gas in most hours to supply the heat demand.

Fig. 14 presents the cooling power supply and demand balance. The expected optimal values of cooling power above and below the horizontal axis illustrate the generation and consumption of the cooling power, respectively. As can be seen in Fig. 14, the cooling demand is met by the chiller and the ISS, so that the chiller is applied at all hours to provide the cooling demand, but in the hours when the cooling demand and the heat market price are high (for example, t = 11–13), it is more economical where part of the cooling demand to be provided by the ISS, in this state the ISS is operated in discharging mode. In Fig. 15, the impact of HSS on the heat market is presented. Based on this figure, due to the presence of HSS, in off-peak hours of heat price (4 to 6), the more heat is purchased from the heat market, and then in peak hours of heat price (10 to 13), the less heat is purchased from the heat market. In Fig. 16, the impact of GSS on the gas market is illustrated. As depicted in this figure, similar to the HSS analysis, the amount of gas bought from the gas market increases at the hours when the gas price is low (4 to 6), and then the value of gas purchased from the gas market decreases at the hours when the gas price is high (7 to 11). In Fig. 17, the effect of ISS on the heat and power market is demonstrated. As mentioned earlier, the ISS meets part of the cooling demand by consuming power, therefore its effects on both the heat and power market. Based on this figure, due to the presence of ISS, the amount of heat bought from the heat market at the heat price peak hours (10 to 13) has decreased, moreover the ISS is purchased its required power during off-peak hours of electricity price (t = 9,10,11,14,15) from the power market. Table 4

4.2.3. The optimal scheduling of water system technologies along with CCHPGW-MG participation in the power market

In this section, according to the optimal solution achieved from solving the multi-objective problem in the first section, the optimal scheduling of water system technologies is investigated. Fig. 18 presents the water network supply and demand balance, per hour. The expected optimal values of water system technologies above and below the horizontal axis illustrate the generation and consumption of the water network, respectively. From the environmental aspect, the SDS has a significant effect on the optimization problem. However, as mentioned earlier, this unit consumes a considerable amount of power, therefore as shown in Fig. 18, the SDS is applied only at electricity price off-peak hours (10 to 15) at its maximum capacity, and other hours, it is much less applied. In addition, the WST pump consumes power when it is in

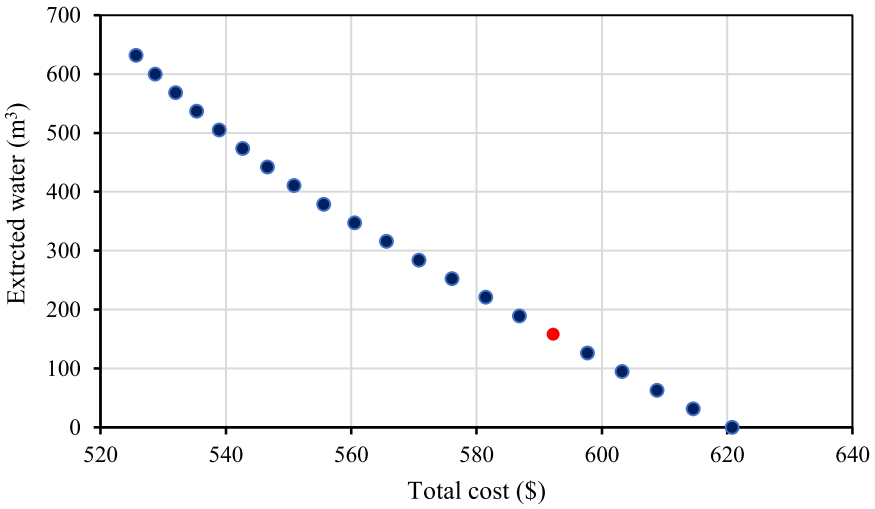

Fig. 8. Pareto optimal solutions to the multi-objective problem.

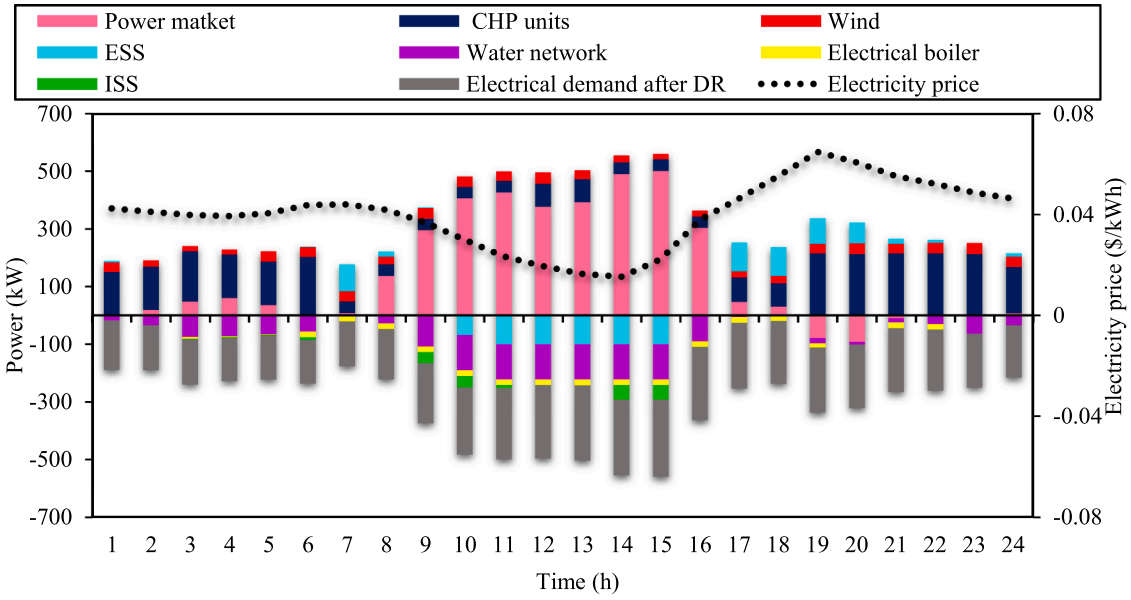

Fig. 9. Electrical power supply and demand balance in the CCHPGW-MG.

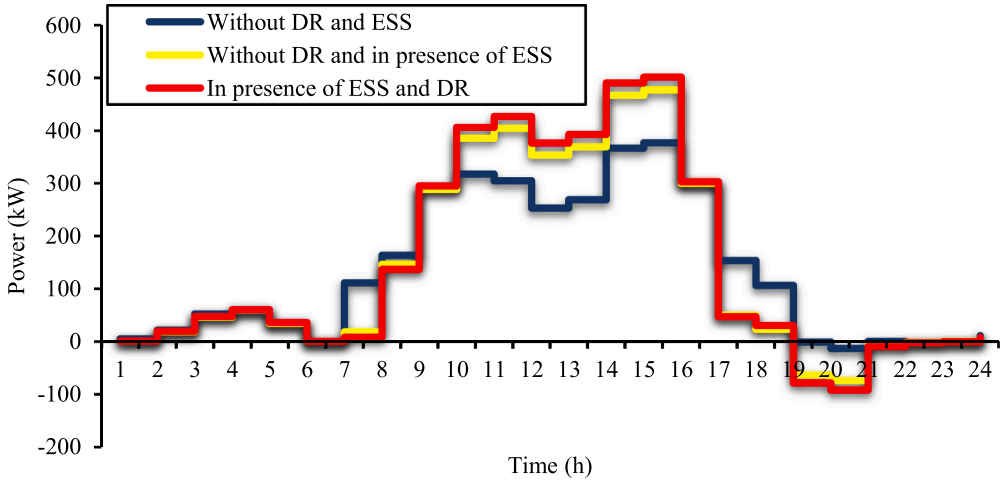

Fig. 10. The impact of ESS and DRP on the power trading with the market.

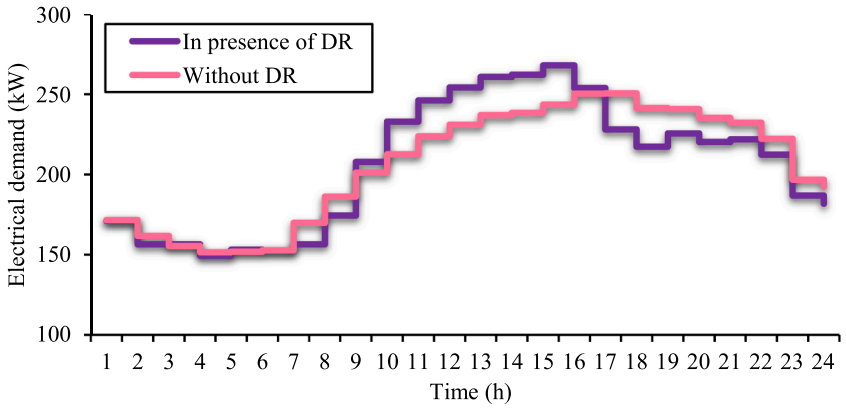

Fig. 11. The variation of electrical demand applying the DR program.

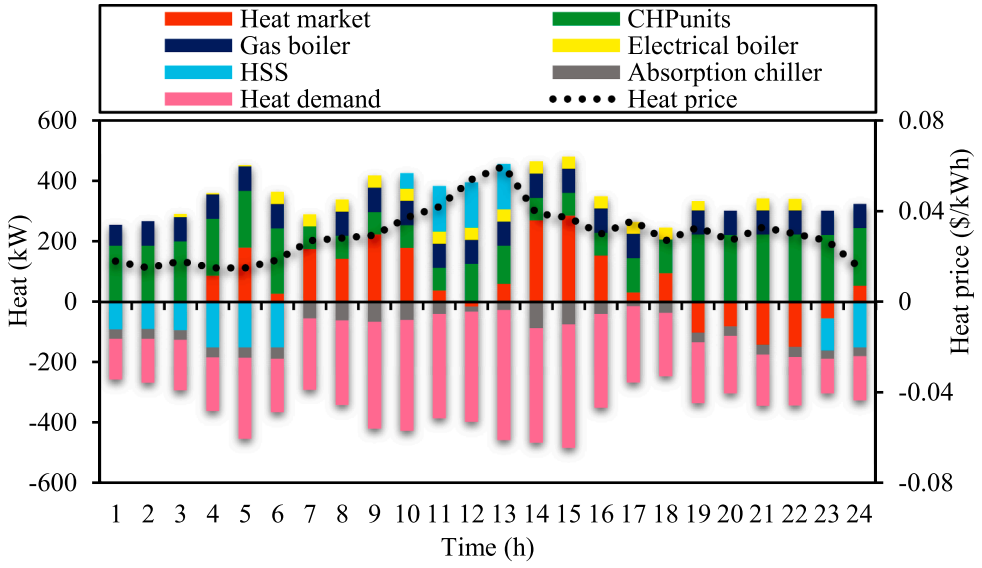

Fig. 12. Heating power supply and demand balance in the CCHPGW-MG.

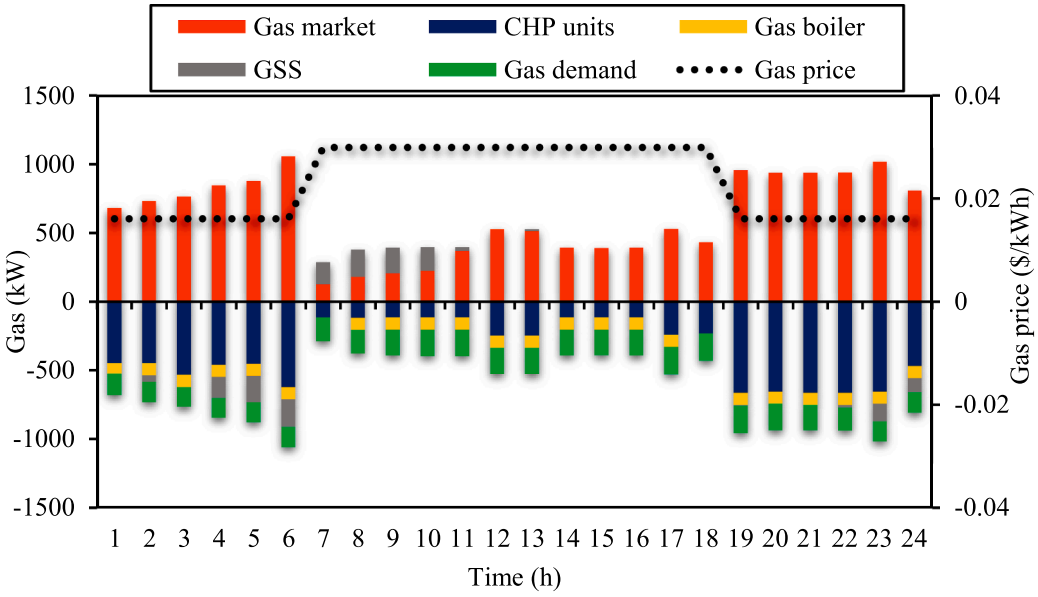

Fig. 13. Gas supply and demand balance in the CCHPGW-MG.

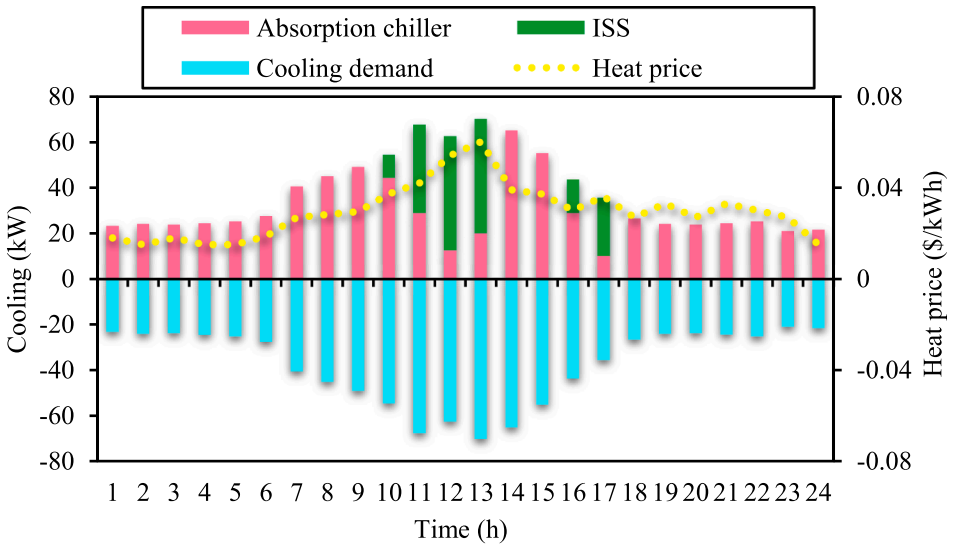

Fig. 14. Cooling power supply and demand balance in the CCHPGW-MG.

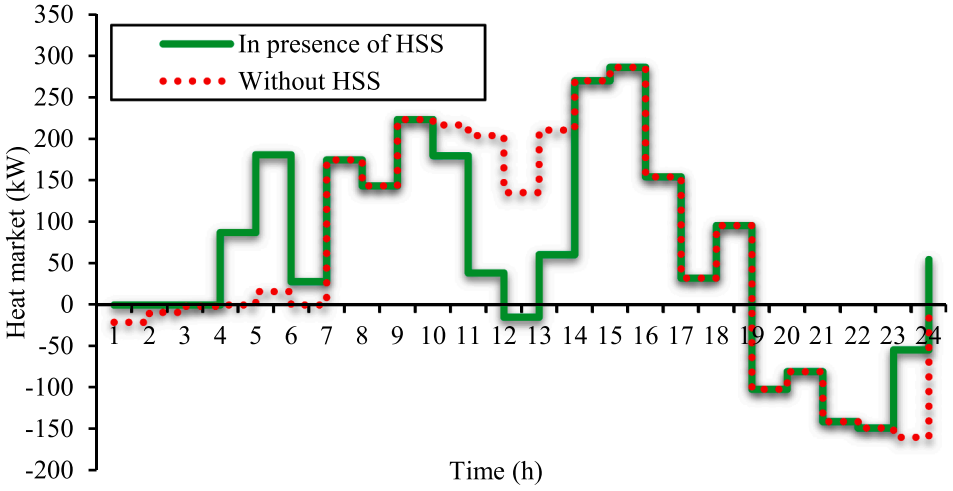

Fig. 15. The impact of HSS on the heat market.

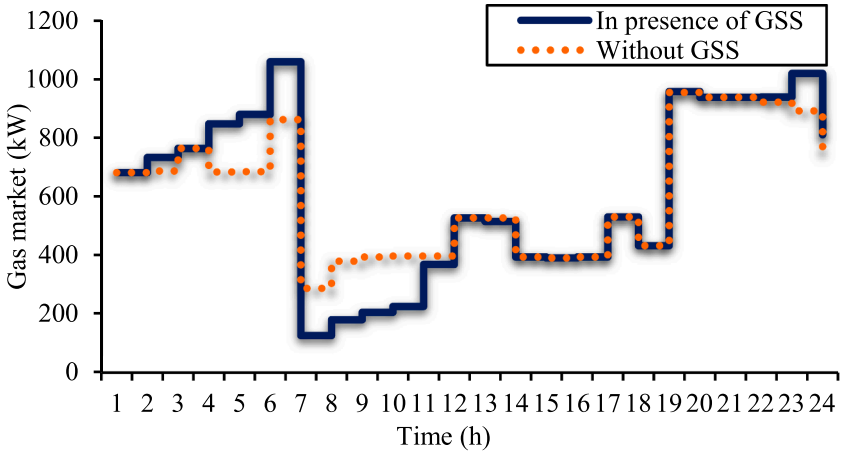

Fig. 16. The impact of GSS on the gas market.

the charging mode, hence the WST is operated during off-peak hours of the electricity price (9 to 16) in the charging mode, and then during peak hours of the electricity market price (17 to 23) in the discharging mode is operated, and accordingly provides part of the water demand. Furthermore, during peak hours of the electricity market price that the use of SDS is not economical; it is more cost-effective to meet water

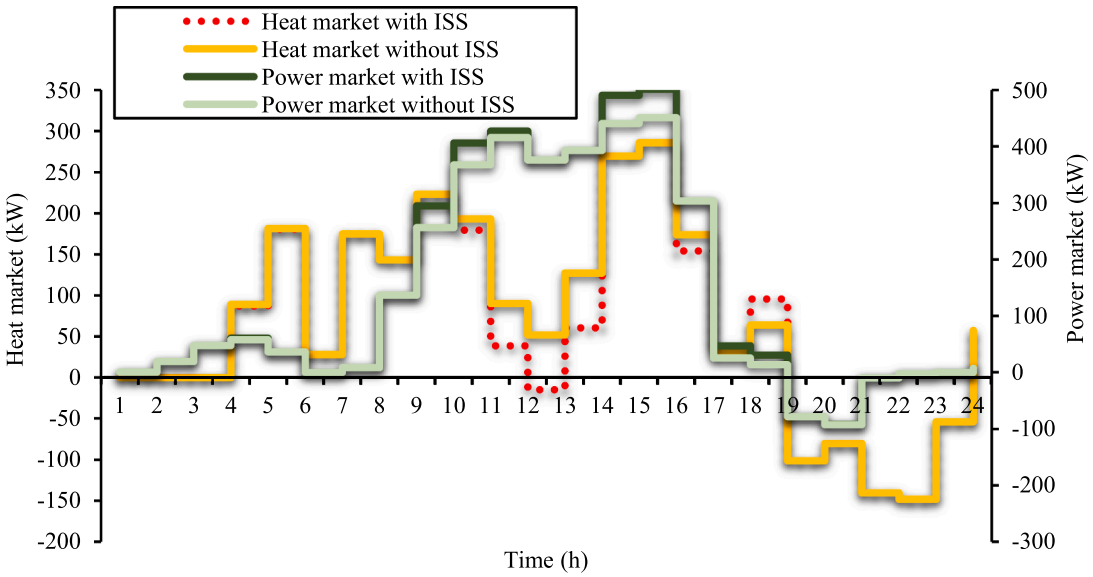

Fig. 17. The impact of ISS on the heat and power market.

Table 4
The occurrence probability of scenarios.

Scenario	W1	W2	W3	W4	W5	W6	W7	W8	W9	W10
Occurrence probability	0.115	0.232	0.044	0.061	0.065	0.015	0.141	0.185	0.116	0.026

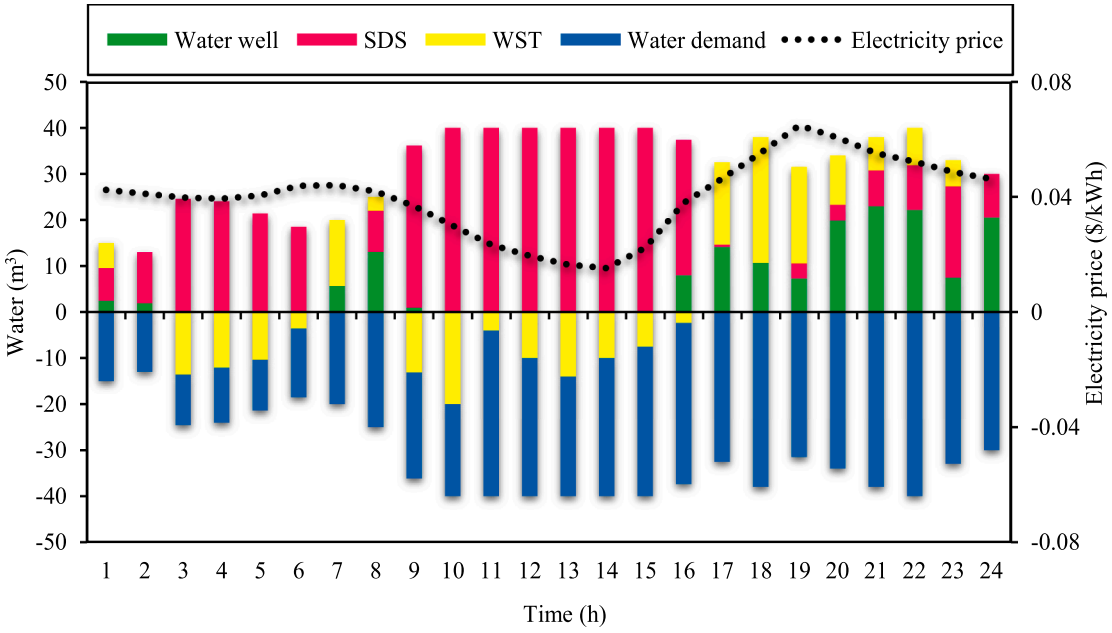

Fig. 18. Water network supply and demand balance in the CCHPGW-MG.

demand via water extracted from the water wells and the WST. Fig. 19 represents the impact of WST on the power market. As can be obvious in this figure, the WST has purchased the power required for its performance during electricity price off-peak hours (for example, 9 to 15) from the power market. Table 5 illustrates the effect of multi-energy storage systems (MESSs), WST and DRP on the total cost. As can be seen from the obtained simulation results, the calculation of the total cost excludes MESSs, WST and DRP is $632.653, while in the presence of MESSs, WST and DRP the total cost is decreased to $592.248, which represents a 6.82% decrement in the total costs of the CCHPGW-MG. Accordingly, it can be resulted that the use of MESSs, WST and DRP have a significant impact on reducing the total cost. Also, according to results obtained from the simulation, WST has decreased the volume of freshwater extracted from water wells from 181.863 m^3 to 157.875 m^3. In addition, with the performed analysis on increasing of adjustable electrical load value up to 20%, the total cost has reduced to $589.640.

In addition, the computational time for the entire system is 21.615 (Second), and the computational time for each part is given in Table 5. The multi-energy microgrids are extremely popular amongst researches at present and some researches have considered various ranges for

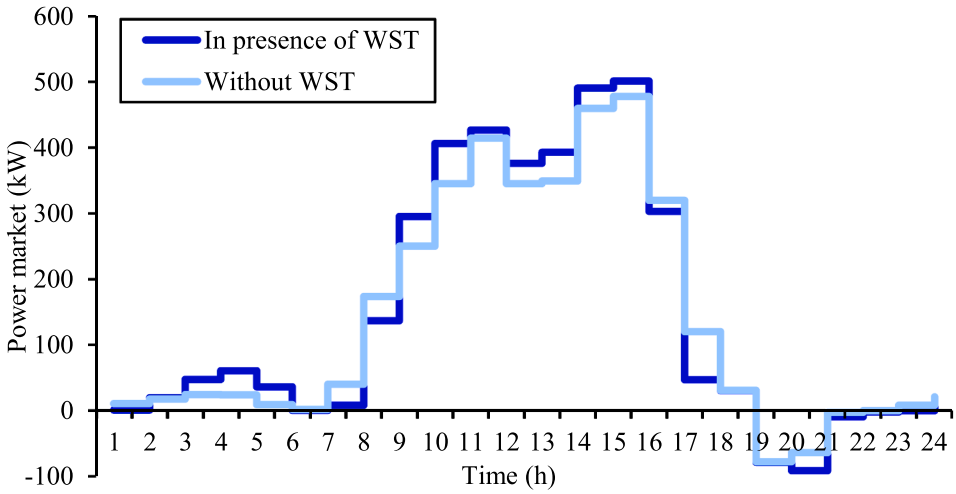

Fig. 19. The impact of WST on the power market.

Table 5
The impact of MESSs, WST and DRP on the total cost and the computational time.

Storages and DR	–	ESS	GSS	HSS	ISS	WST	DR	Multi-energy storages and DR
Total cost ($) (Operating cost and emission cost)	632.653	620.790	623.941	625.962	626.757	626.778	629.088	592.248
computational time (Second)	03:012	04.563	03.941	03.570	05.345	06.697	03.924	21.615

microgrids as kW (e.g., 160 kW-700 kW) and as MW (e.g., by 45 MW) (Is there any specific power rating what kW or MW for microgrid, n.d.). Therefore, it is clear that the renewable energy microgrids can be utilized as the large-scale microgrids. For example, (He, Zhang, Chen, Ren & Li, 2018) can be introduced as a practical sample, in which the renewable energy microgrid with the photovoltaic system, wind turbine, electrical storage systems and power convertor in the large-scale has been proposed. These results are concluded that the large-scale microgrid can be implemented by the proposed work.

5. Conclusion

This paper proposed an optimal scheduling model for a developed microgrid named combined cooling, heating, power, gas and water-based microgrid (CCHPGW-MG). A multi-objective optimization problem was introduced to minimize the operating cost, emission cost, and freshwater volume extracted from water wells, which was solved via the epsilon constraint method. The prime reason to design the multi-objective problem was the opposite behaviour to minimize the energy cost besides water production via seawater desalination system (SDS). In this study, two main aspects were investigated. The first aspect was related to environmental and economic issues, and the second aspect was focused on the underground reservoirs of the potable water and water crisis. Furthermore, a two-stage stochastic approach was applied to manage the uncertainties related to the electrical load, wind power and electricity price in the CCHPGW-MG. The use of seawater desalination system (SDS) technology not only cause to reduce environmental pollution but also decrease the extraction of potable water from underground reservoirs. Since the SDS consumes a significant amount of power for its performance, the water storage tank (WST) was applied to meet part of the water demand during electricity price peak hours to reduce total cost. The role of MESSs such as electrical storage system (ESS), heat storage system (HSS), gas storage system (GSS), ice storage system (ISS) and water storage tank (WST), as well as the DRP have been investigated on the operation of the integrated model. By simultaneously considering water system technologies such as SDS, WST, and water well, not only has been decreased the volume of freshwater extracted from water wells, but also from economic and environmental aspects is affected the optimal operating of the presented model. In particular, the optimal operation of the water sector technologies would enhance the optimal operation of the energy systems to benefit the entire system. The numerical results illustrated the following points:

1) Multi-energy storage systems, WST along with DR program, have been reduced the total cost, including operating cost and emission cost, by 6.82%.
2) WST has been decreased the value of potable water extracted from water wells by 15.2%.
3) The integrated scheduling model of the energy-water system, in addition to the total cost reduction, has been reduced the volume of freshwater extracted from underground reservoirs by 64%.

Declaration of Competing Interest

This manuscript has not been submitted to, nor is under review at, another journal or other publishing venue.

References

Agabalaye-Rahvar, M., Mansour-Saatloo, A., Mirzaei, M. A., Mohammadi-Ivatloo, B., & Zare, K. (2021). Economic-environmental stochastic scheduling for hydrogen storage-based smart energy hub coordinated with integrated demand response program. *International Journal of Energy Research*.

Ahmadi, E., McLellan, B., Ogata, S., Mohammadi-Ivatloo, B., & Tezuka, T. (2020). An integrated planning framework for sustainable water and energy supply. *Sustainability, 12*(10), 4295.

Ahrabi, M., Abedi, M., Nafisi, H., Mirzaei, M. A., Mohammadi-Ivatloo, B., & Marzband, M. (2021). Evaluating the effect of electric vehicle parking lots in transmission-constrained AC unit commitment under a hybrid IGDT-stochastic approach. *International Journal of Electrical Power & Energy Systems, 125*, Article 106546.

Amir, V., & Azimian, M. (2020). Dynamic multi-carrier microgrid deployment under uncertainty. *Applied Energy, 260*, Article 114293.

Caldera, U., Bogdanov, D., & Breyer, C. (2016). Local cost of seawater RO desalination based on solar PV and wind energy: A global estimate. *Desalination, 385*, 207–216.

Cui, Q., Ma, P., Huang, L., Shu, J., Luv, J., & Lu, L. (2020). Effect of device models on the multiobjective optimal operation of CCHP microgrids considering shiftable loads. *Applied Energy, 275*, Article 115369.

Dai, J., Wu, S., Han, G., Weinberg, J., Xie, X., Wu, X., et al. (2018). Water-energy nexus: A review of methods and tools for macro-assessment. *Applied Energy, 210*, 393–408.

Daneshvar, M., Mohammadi-Ivatloo, B., Asadi, S., Anvari-Moghaddam, A., Rasouli, M., Abapour, M. B., et al. (2020). Chance-constrained models for transactive energy management of interconnected microgrid clusters. *Journal of Cleaner Production*, 271.

Ding, X., Guo, Q., Qiannan, T., & Jermsittiparsert, K. (2021). Economic and environmental assessment of multi-energy microgrids under a hybrid optimization technique. *Sustainable Cities and Society, 65*, Article 102630.

Ehsan, A., & Yang, Q. (2019). Scenario-based investment planning of isolated multi-energy microgrids considering electricity, heating and cooling demand. *Applied Energy, 235*, 1277–1288.

Fateh, H., Bahramara, S., & Safari, A. (2020). Modeling operation problem of active distribution networks with retailers and microgrids: A multi-objective bi-level approach. *Applied Soft Computing, 94*, Article 106484.

Feizizadeh, B., Ronagh, Z., Pourmoradian, S., Gheshlaghi, H. A., Lakes, T., & Blaschke, T. (2021). An efficient GIS-based approach for sustainability assessment of urban drinking water consumption patterns: A study in Tabriz city. *Iran. Sustainable Cities and Society, 64*, Article 102584.

Hadayeghparast, S., Farsangi, A. S., & Shayanfar, H. (2019). Day-ahead stochastic multi-objective economic/emission operational scheduling of a large scale virtual power plant. *Energy, 172*, 630–646.

He, L., Zhang, S., Chen, Y., Ren, L., & Li, J. (2018). Techno-economic potential of a renewable energy-based microgrid system for a sustainable large-scale residential community in Beijing. *China. Renewable and Sustainable Energy Reviews, 93*, 631–641.

Hemmati, M., Mohammadi-Ivatloo, B., Abapour, M., & Anvari-Moghaddam, A. (2020). Optimal chance-constrained scheduling of reconfigurable microgrids considering islanding operation constraints. *IEEE Systems Journal*.

Hemmati, M., Mohammadi-Ivatloo, B., Ghasemzadeh, S., & Reihani, E. (2018). Risk-based optimal scheduling of reconfigurable smart renewable energy based microgrids. *International Journal of Electrical Power & Energy Systems, 101*, 415–428.

Hou, H., Xue, M., Xu, Y., Xiao, Z., Deng, X., Xu, T., et al. (2020). Multi-objective economic dispatch of a microgrid considering electric vehicle and transferable load. *Applied Energy, 262*, Article 114489.

Jahani, A., Zare, K., Khanli, L. M., & Karimipour, H. (2021). Optimized power trading of reconfigurable microgrids in distribution energy market. *IEEE access : practical innovations, open solutions, 9*, 48218–48235.

Jalilian, F., Mansour-Saatloo, A., Mirzaei, M. A., Mohammadi-Ivatloo, B., & Zare, K. (2021). *Optimal participation of electric vehicles aggregator in energy and flexible ramping markets, energy storage in energy markets* (pp. 217–233). Elsevier.

Li, M., Fu, Q., Singh, V. P., Ji, Y., Liu, D., Zhang, C., et al. (2019). An optimal modelling approach for managing agricultural water-energy-food nexus under uncertainty. *Science of the Total Environment, 651*, 1416–1434.

Li, Q., Yu, S., Al-Sumaiti, A. S., & Turitsyn, K. (2018). Micro water–energy nexus: Optimal demand-side management and quasi-convex hull relaxation. *IEEE Transactions on Control of Network Systems, 6*(4), 1313–1322.

Li, Z., & Xu, Y. (2019). Temporally-coordinated optimal operation of a multi-energy microgrid under diverse uncertainties. *Applied Energy, 240*, 719–729.

Mansour-Saatloo, A., Agabalaye-Rahvar, M., Mirzaei, M. A., Mohammadi-Ivatloo, B., Abapour, M., & Zare, K. (2020a). Robust scheduling of hydrogen based smart micro energy hub with integrated demand response. *Journal of Cleaner Production, 267*, Article 122041.

Mansour-Saatloo, A., Mirzaei, M. A., Mohammadi-Ivatloo, B., & Zare, K. (2020b). A risk-averse hybrid approach for optimal participation of power-to-hydrogen technology-based multi-energy microgrid in multi-energy markets. *Sustainable Cities and Society, 63*, Article 102421.

Mirzaei, M. A., Hemmati, M., Zare, K., Abapour, M., Mohammadi-Ivatloo, B., Marzband, M., et al. (2020a). A novel hybrid two-stage framework for flexible bidding strategy of reconfigurable micro-grid in day-ahead and real-time markets. *International Journal of Electrical Power & Energy Systems, 123*, Article 106293.

Mirzaei, M. A., Oskouei, M. Z., Mohammadi-Ivatloo, B., Loni, A., Zare, K., Marzband, M., et al. (2020b). Integrated energy hub system based on power-to-gas and compressed air energy storage technologies in the presence of multiple shiftable loads. *IET Generation, Transmission & Distribution, 14*(13), 2510–2519.

Mirzaei, M. A., Zare, K., Mohammadi-Ivatloo, B., Marzband, M., & Anvari-Moghaddam, A. (2021). Robust network-constrained energy management of a multiple energy distribution company in the presence of multi-energy conversion and storage technologies. *Sustainable Cities and Society, 74*, Article 103147.

Moazeni, F., & Khazaei, J. (2020a). Dynamic economic dispatch of islanded water-energy microgrids with smart building thermal energy management system. *Applied Energy, 276*, Article 115422.

Moazeni, F., & Khazaei, J. (2020b). Optimal operation of water-energy microgrids; a mixed integer linear programming formulation. *Journal of Cleaner Production, 275*, Article 122776.

Moazeni, F., & Khazaei, J. (2021). Optimal energy management of water-energy networks via optimal placement of pumps-as-turbines and demand response through water storage tanks. *Applied Energy, 283*, Article 116335.

Moazeni, F., Khazaei, J., & Mendes, J. P. P. (2020). Maximizing energy efficiency of islanded micro water-energy nexus using co-optimization of water demand and energy consumption. *Applied Energy, 266*, Article 114863.

Murillo-Sánchez, C. E., Zimmerman, R. D., Anderson, C. L., & Thomas, R. J. (2013). Secure planning and operations of systems with stochastic sources, energy storage, and active demand. *IEEE Transactions on Smart Grid, 4*(4), 2220–2229.

Murty, V., & Kumar, A. (2020). Multi-objective energy management in microgrids with hybrid energy sources and battery energy storage systems. *Protection and Control of Modern Power Systems, 5*(1), 1–20.

Najafi, J., Peiravi, A., Anvari-Moghaddam, A., & Guerrero, J. M. (2019). Resilience improvement planning of power-water distribution systems with multiple microgrids against hurricanes using clean strategies. *Journal of cleaner production, 223*, 109–126.

Nami, H., Anvari-Moghaddam, A., & Arabkoohsar, A. (2020). Application of CCHPs in a centralized domestic heating, cooling and power network—Thermodynamic and economic implications. *Sustainable Cities and Society, 60*, Article 102151.

Nasiri, N., Yazdankhah, A. S., Mirzaei, M. A., Loni, A., Mohammadi-Ivatloo, B., Zare, K., et al. (2020). A bi-level market-clearing for coordinated regional-local multi-carrier systems in presence of energy storage technologies. *Sustainable Cities and Society, 63*, Article 102439.

Nazari-Heris, M., Abapour, S., & Mohammadi-Ivatloo, B. (2017). Optimal economic dispatch of FC-CHP based heat and power micro-grids. *Applied Thermal Engineering, 114*, 756–769.

Nazari-Heris, M., Mirzaei, M. A., Mohammadi-Ivatloo, B., Marzband, M., & Asadi, S. (2020). Economic-environmental effect of power to gas technology in coupled electricity and gas systems with price-responsive shiftable loads. *Journal of Cleaner Production, 244*, Article 118769.

Oskouei, M. Z., Mirzaei, M. A., Mohammadi-Ivatloo, B., Shafiee, M., Marzband, M., & Anvari-Moghaddam, A. (2021). A hybrid robust-stochastic approach to evaluate the profit of a multi-energy retailer in tri-layer energy markets. *Energy, 214*, Article 118948.

Pakdel, M. J. V., Sohrabi, F., & Mohammadi-Ivatloo, B. (2020). Multi-objective optimization of energy and water management in networked hubs considering transactive energy. *Journal of Cleaner Production*, Article 121936.

Pourghasem, P., Sohrabi, F., Abapour, M., & Mohammadi-Ivatloo, B. (2019). Stochastic multi-objective dynamic dispatch of renewable and CHP-based islanded microgrids. *Electric Power Systems Research, 173*, 193–201.

Roustaei, M., Niknam, T., Salari, S., Chabok, H., Sheikh, M., Kavousi-Fard, A., et al. (2020). A scenario-based approach for the design of Smart Energy and Water Hub. *Energy, 195*.

Saberi, K., Pashaei-Didani, H., Nourollahi, R., Zare, K., & Nojavan, S. (2019). Optimal performance of CCHP based microgrid considering environmental issue in the presence of real time demand response. *Sustainable cities and society, 45*, 596–606.

Shang, Y., Hei, P., Lu, S., Shang, L., Li, X., Wei, Y., et al. (2018). China's energy-water nexus: Assessing water conservation synergies of the total coal consumption cap strategy until 2050. *Applied Energy, 210*, 643–660.

Sui, Q., Wei, F., Lin, X., & Li, Z. (2021). Optimal energy management of a renewable microgrid integrating water supply systems. *International Journal of Electrical Power & Energy Systems, 125*, Article 106445.

Wang, X.-. C., Jiang, P., Yang, L., Van Fan, Y., Klemeš, J. J., & Wang, Y. (2021). Extended water-energy nexus contribution to environmentally-related sustainable development goals. *Renewable and Sustainable Energy Reviews, 150*, Article 111485.

Wang, X.-. C., Klemeš, J. J., Wang, Y., Dong, X., Wei, H., Xu, Z., et al. (2020a). Water-energy-carbon emissions nexus analysis of China: An environmental input-output model-based approach. *Applied Energy, 261*, Article 114431.

Wang, Y., Tang, L., Yang, Y., Sun, W., & Zhao, H. (2020b). A stochastic-robust coordinated optimization model for CCHP micro-grid considering multi-energy operation and power trading with electricity markets under uncertainties. *Energy*, Article 117273.

Wei, J., Zhang, Y., Wang, J., Cao, X., & Khan, M. A. (2020a). Multi-period planning of multi-energy microgrid with multi-type uncertainties using chance constrained information gap decision method. *Applied Energy, 260*, Article 114188.

Wei, J., Zhang, Y., Wang, J., Cao, X., & Khan, M. A. (2020b). Multi-period planning of multi-energy microgrid with multi-type uncertainties using chance constrained information gap decision method. *Applied Energy*, 260.

Wu, Y., Wang, X., Fu, Y., & Xu, Y. (2017). *Difference brain storm optimization for combined heat and power economic dispatch, international conference on swarm intelligence* (pp. 519–527). Springer.

Yang, Y., Tang, L., Wang, Y., & Sun, W. (2020). Integrated operation optimization for CCHP micro-grid connected with power-to-gas facility considering risk management and cost allocation. *International Journal of Electrical Power & Energy Systems, 123*, Article 106319.

Zhang, W., Valencia, A., Gu, L., Zheng, Q. P., & Chang, N.-. B. (2020). Integrating emerging and existing renewable energy technologies into a community-scale microgrid in an energy-water nexus for resilience improvement. *Applied Energy, 279*, Article 115716.

Zhou, Y., Shahidehpour, M., Wei, Z., Li, Z., Sun, G., & Chen, S. (2019). Distributionally robust unit commitment in coordinated electricity and district heating networks. *IEEE Transactions on Power Systems, 35*(3), 2155–2166.